2017-03

Environmental degradation of structured nanocomposites

Rockford, Stephanie M.

Monterey, California: Naval Postgraduate School

NAVAL POSTGRADUATE SCHOOL

MONTEREY, CALIFORNIA

THESIS

ENVIRONMENTAL DEGRADATION OF STRUCTURED NANOCOMPOSITES

by

Stephanie M. Rockford

March 2017

Thesis Advisor: Claudia Luhrs
Second Reader: Sarath Menon

Approved for public release. Distribution is unlimited.

THIS PAGE INTENTIONALLY LEFT BLANK

REPORT DOCUMENTATION PAGE			*Form Approved OMB No. 0704–0188*
Public reporting burden for this collection of information is estimated to average 1 hour per response, including the time for reviewing instruction, searching existing data sources, gathering and maintaining the data needed, and completing and reviewing the collection of information. Send comments regarding this burden estimate or any other aspect of this collection of information, including suggestions for reducing this burden, to Washington headquarters Services, Directorate for Information Operations and Reports, 1215 Jefferson Davis Highway, Suite 1204, Arlington, VA 22202-4302, and to the Office of Management and Budget, Paperwork Reduction Project (0704-0188) Washington, DC 20503.			
1. AGENCY USE ONLY ***(Leave blank)***	**2. REPORT DATE** March 2017	**3. REPORT TYPE AND DATES COVERED** Master's thesis	
4. TITLE AND SUBTITLE ENVIRONMENTAL DEGRADATION OF STRUCTURED NANOCOMPOSITES			**5. FUNDING NUMBERS**
6. AUTHOR(S) Stephanie M. Rockford			
7. PERFORMING ORGANIZATION NAME(S) AND ADDRESS(ES) Naval Postgraduate School Monterey, CA 93943-5000			**8. PERFORMING ORGANIZATION REPORT NUMBER**
9. SPONSORING /MONITORING AGENCY NAME(S) AND ADDRESS(ES) N/A			**10. SPONSORING / MONITORING AGENCY REPORT NUMBER**
11. SUPPLEMENTARY NOTES The views expressed in this thesis are those of the author and do not reflect the official policy or position of the Department of Defense or the U.S. Government. IRB number ____N/A____.			
12a. DISTRIBUTION / AVAILABILITY STATEMENT Approved for public release. Distribution is unlimited.			**12b. DISTRIBUTION CODE**

13. ABSTRACT (maximum 200 words)

Epoxy resin nanocomposites are currently being used in multiple structural and multifunctional applications. However, the amount of data known regarding their degradation due to atmospheric conditions (UV light, humidity, temperature) is very limited. This study aims to characterize the change in properties as result of environmental factors by examining the effects suffered by epoxy resins containing nano-fillers when exposed to augmented weather conditions. To achieve that goal, neat epoxy resin specimens and epoxy resin samples loaded with 1% of carbon nanotubes, silica nanoparticles, nickel or nickel/nickel oxide nano-powder were fabricated, and their properties compared. The samples were exposed to three cycles, totaling 246 hours, of UV light and humidity in a QUV accelerated weather chamber and to salt spray in a salt fog chamber. After each exposure cycle, the samples were characterized using optical microscopy, microhardness tests, tensile tests, scanning electron microscopy, and Fourier transform infrared spectroscopy. The specimen's electrical conductivity was measured using a four-point probe. The sample analysis after exposure showed changes in the nanocomposite surface structure and microstructure-increase in hardness; loss of ultimate tensile strength, in particular for the carbon nanotube composite; and dramatic changes in the Young's modulus among all samples but little change to their sheet resistance. The nanocomposite formulations were also deposited on the surface of 315L stainless steel shim to determine the effects of the augmented weather conditions in the epoxy nanocomposite-metallic pair. Recommendations for future research include examining various composite loadings, developing protocols to achieve better dispersion of fillers on the resin and lengthening exposure times.

14. SUBJECT TERMS nanocomposite, nano, nanotubes, CNT, MWCNT, carbon, nickel, nickel oxide, epoxy, UV, humidity, condensation, salt fog, degradation, exposure			**15. NUMBER OF PAGES** 87
			16. PRICE CODE
17. SECURITY CLASSIFICATION OF REPORT Unclassified	**18. SECURITY CLASSIFICATION OF THIS PAGE** Unclassified	**19. SECURITY CLASSIFICATION OF ABSTRACT** Unclassified	**20. LIMITATION OF ABSTRACT** UU

NSN 7540–01-280-5500 Standard Form 298 (Rev. 2–89)
Prescribed by ANSI Std. 239–18

THIS PAGE INTENTIONALLY LEFT BLANK

Approved for public release. Distribution is unlimited.

ENVIRONMENTAL DEGRADATION OF STRUCTURED NANOCOMPOSITES

Stephanie M. Rockford
Lieutenant, United States Navy
B.S., United States Naval Academy, 2010

Submitted in partial fulfillment of the
requirements for the degree of

MASTER OF SCIENCE IN MECHANICAL ENGINEERING

from the

NAVAL POSTGRADUATE SCHOOL
March 2017

Approved by: Claudia Luhrs
Thesis Advisor

Sarath Menon
Second Reader

Garth Hobson
Chair, Department of Mechanical and Aerospace Engineering

THIS PAGE INTENTIONALLY LEFT BLANK

ABSTRACT

Epoxy resin nanocomposites are currently being used in multiple structural and multifunctional applications. However, the amount of data known regarding their degradation due to atmospheric conditions (UV light, humidity, temperature) is very limited. This study aims to characterize the change in properties as result of environmental factors by examining the effects suffered by epoxy resins containing nano-fillers when exposed to augmented weather conditions. To achieve that goal, neat epoxy resin specimens and epoxy resin samples loaded with 1% of carbon nanotubes, silica nanoparticles, nickel or nickel/nickel oxide nano-powder were fabricated, and their properties compared. The samples were exposed to three cycles, totaling 246 hours, of UV light and humidity in a QUV accelerated weather chamber and to salt spray in a salt fog chamber. After each exposure cycle, the samples were characterized using optical microscopy, microhardness tests, tensile tests, scanning electron microscopy, and Fourier transform infrared spectroscopy. The specimen's electrical conductivity was measured using a four-point probe. The sample analysis after exposure showed changes in the nanocomposite surface structure and microstructure-increase in hardness; loss of ultimate tensile strength, in particular for the carbon nanotube composite; and dramatic changes in the Young's modulus among all samples but little change to their sheet resistance. The nanocomposite formulations were also deposited on the surface of 315L stainless steel shim to determine the effects of the augmented weather conditions in the epoxy nanocomposite-metallic pair. Recommendations for future research include examining various composite loadings, developing protocols to achieve better dispersion of fillers on the resin and lengthening exposure times.

THIS PAGE INTENTIONALLY LEFT BLANK

TABLE OF CONTENTS

LIST OF FIGURES

THIS PAGE INTENTIONALLY LEFT BLANK

LIST OF TABLES

THIS PAGE INTENTIONALLY LEFT BLANK

LIST OF ACRONYMS AND ABBREVIATIONS

CNT	carbon nanotubes
DOD	Department of Defense
FTIR	Fourier Transform Infrared Spectroscopy
IR	infrared
MWCNT	multiwall carbon nanotubes
Ni	nickel
Ni/NiO	nickel/nickel oxide
nm	nanometer
NPS	Naval Postgraduate School
SEM	scanning electron microscope
SiO_2	silicon dioxide
SWCNT	single-wall carbon nanotubes
TGA	Thermogravimetric Analysis
UTS	Ultimate Tensile Strength
UV	ultraviolet
XRD	X-ray diffraction
μm	micrometer

THIS PAGE INTENTIONALLY LEFT BLANK

ACKNOWLEDGMENTS

I would like to thank my thesis advisor, Professor Claudia Luhrs, for encouraging my interest in material science and introducing me to the field of nanomaterials. Prof. Luhrs was always available, and her guidance was indispensable throughout my research.

I would also like to thank Professor Sarath Menon, Professor Hugo Zea, Dr. Chanman Park, Dr. William Wu, and Mr. John Mobley. Their expertise, patience and input helped me immensely during this process. I also would like to thank Gunnar Kozel and Camden Webb for their tireless efforts and long hours helping fabricate samples, which allowed me to process and analyze data under a tight deadline.

I would also like to acknowledge the Corrosion Policy and Oversight Office for their interest and financial support, which allowed me to conduct this research.

Finally, I would like to thank my husband, Chris, and son, Hunter, for providing me encouragement and support for the past two years.

THIS PAGE INTENTIONALLY LEFT BLANK

I. INTRODUCTION

A. MOTIVATION

Nanocomposites have a variety of applications in defense systems such as anticorrosive coatings, structural materials for harder/lighter platforms, stealth systems, sensors, electrical components and alternative energy systems among others [1]. As an example of systems containing nanocomposites, Figure 1 presents the F-35A Lightning II Manufactured by Lockheed Martin, first mass-produced aircraft to include carbon nanotube reinforced epoxy resins. Nanocomposites can have increased hardness and elastic modulus, lower wear rates and higher thermal stability [2]-[6]. In addition, nanocomposites have an exceptionally high surface to volume ratio, which changes the matrix properties in the vicinity of the filler phase.

Figure 1. F-35A Lightning II Manufactured by Lockheed Martin. Source: [7].

In order to gain a full understanding of the variables that affect the life cycle of systems that contain nanocomposites, it becomes indispensable to characterize the change in properties that nanocomposites suffer due to environmental factors. Therefore, this research was motivated by the realization that there is very limited data published concerning epoxy-based nanocomposites' aging or degradation due to cycles in UV light, temperature and humidity. The study herein aims to quantify the effects that some cycles in a simulated weather environment have in neat epoxy specimens and in epoxy

nanocomposites fabricated using multiwall carbon nanotubes (MWCNT), silica dioxide (SiO_2), nickel (Ni) and nickel/nickel oxide (Ni/NiO) nanoparticles.

B. BACKGROUND

Reinforcing polymers with filler materials has become a common practice in production of plastics; however, the use of polymer nanocomposites only started to receive significant attention and gain prominence in the research community since the discovery of carbon nanotubes (CNT). A polymeric composite is considered to be a nanocomposite when the filler used has at least one feature (length, diameter, thickness, etc.) in the nanometer scale [1]. A nanofiller could present a variety of shapes; some common profiles are shown in Figure 2.

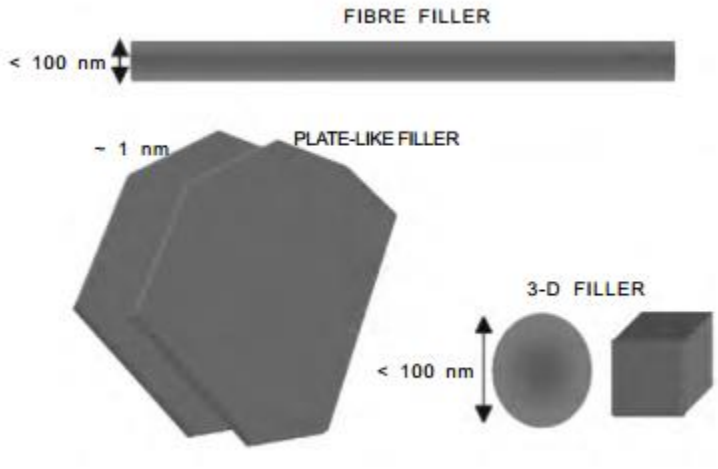

Figure 2. Common Filler Shapes on the Nanoscale. Source: [1].

Nanomaterials have an increased surface area on the order of 10^7 (Figure 3. The larger surface area of the nanofiller results in an increase in the interfacial region in the nanocomposite. The size of the interfacial region determines the amount at which the filler characteristics are transferred to the composite. Kurahatti [1] reported that the interfacial region can be as small as 2nm. As a result, the composite will have altered and improved characteristics relating to the nanofiller chosen.

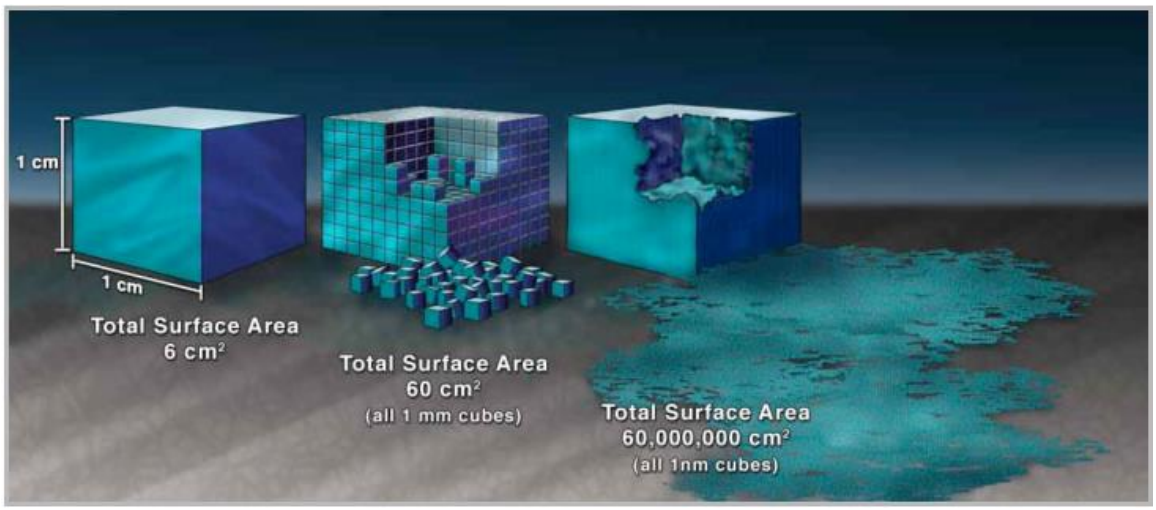

Figure 3. Illustration of Surface Area for Various Size Particles Including Nanocubes. Source: [8].

In 1991, Iijima [9] published a paper documenting creation of CNTs. Since this time, interest in CNTs and other nanomaterials has increased and the research has diversified [9]. Extensive research has been conducted examining preparation methods, and documenting varying mechanical, compositional and structural characteristics. Numerous publications highlight the use of CNT as fillers in polymeric matrices; however, there is limited research addressing the effect of environmental factors on the degradation of such nanocomposites. Department of Defense (DOD) applications of nanocomposites, particularly those used in marine environments, would inherently face harsh weather conditions such as ultraviolet (UV) radiation, humidity, widely varying temperatures and corrosive environments.

A literature review into environmental degradation of nanocomposites highlights, although not necessarily quantifies, some of the expected negative outcomes of exposing samples to diverse conditions. For example, Ging et al. [10] present the environmental and toxicological implications of the release of nanocomposites although do not present a detail study of their degradation. Asmatulu et al. [11] and Nguyen at al. [12] review the adverse effects of UV radiation in the CNT composite coatings. Yousif and Haddad [13] studied polystyrene, finding that UV radiation causes photo oxidative degradation, which results in breakage of the polymeric chains, generation of radical species and reduction in

the molecular weight. All of those have detrimental effects on mechanical properties and lead to what the authors describe as “useless materials, after an unpredictable time” [13]. Bottino et al. [14] showed that within 24 hours of UV exposure, polystyrene had a significant decrease in mechanical data. Concerning epoxy resins, research into carbon fiber-reinforced epoxy by Kumar et al. [15], using micron size fibers, showed that concurrent UV radiation and humidity exposure causes “matrix erosion, matrix microcracking, fiber debonding, fiber loss and void formation.” The conclusion of such study was that bare polymeric matrices and traditional carbon fiber reinforced composites will degrade after UV and humidity exposure, which will ultimately degrade their performance [15]. Other reports, as the one published by Bocchini et al. [16], support the findings that UV wavelengths between 290–400 nm create free radicals in polymer molecules that degrade the quality of polymers and are expected to have the same effect in nanocomposites. In addition, water absorption can cause polymer matrices to swell, reducing the mechanical strength and promoting blistering [16].

In this study, epoxy resin was chosen as the bare matrix for analysis and eventual nanomaterial loading. Epoxy resins are thermosetting materials and consist of a resin and hardener. Epoxy resins are used in paints, coatings, adhesives, industrial tooling, electrical systems, and marine applications. The chemical structure of epoxy formulations varies and include a chemical reaction between one or two monomers. All epoxies do have an epoxy monomer in common. An epoxy monomer constitutes a three-member ring between two carbons and one oxygen atom known as an oxirane functional group. According to Gonzales [17], “this atomic arrangement shows enhanced reactivity when compared with common ethers because of its high strain” and because oxygen and carbon have different electronegativity, this “causes polarity of the oxirane ring” and it can be detected using infrared (IR) spectroscopy. The oxirane ring can be seen in Figure 4.

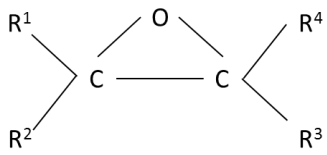

Figure 4. Oxirane Ring. Source: [17].

In this study, SpeciFix and EpoFix (Struers), two part epoxy resins were used and have the structure seen in Figure 5. Both SpeciFix and EpoFix are bisephenol-A-(epichlorhydrin).

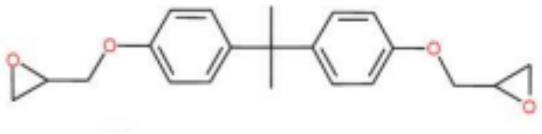

Figure 5. 2,2-Bis[4-(glycidyloxy)phenyl]propane (DGEBA). Source: [17].

As previously mentioned, Iijima is credited with discovering CNT's, both single walled carbon nanotubes (SWCNT) and MWCNTS. A schematic of SWCNT and MWCNT can be found in Figure 6. CNTs, like all nanomaterials, have one dimension on the nanoscale 1–100nm. The diameter of a CNT is less than 100nm while the length of the tubes can reach 1µm. The tubes consist of covalently bonded carbon atoms. Since Iijima's discovery, there have been increasing interest and research into CNT's and their use in composites. Loos et al. [18] used SWCNT dispersed in acetone then added to an epoxy resin before curing. The research found that the IR analysis for the cured nanocomposite and neat epoxy were slightly different. Also, tensile tests conducted in the study showed an increase in Young's modulus and strength for the composite [18].This research did not expose the samples to UV light or humidity but did show the improved performance of nanocomposites using CNTs.

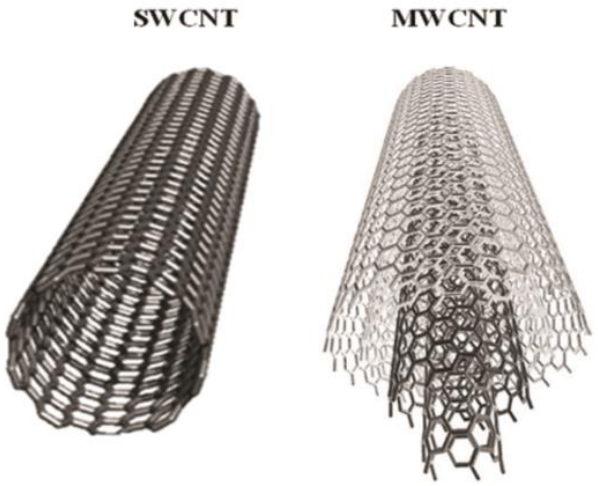

Figure 6. Schematic of Single Wall Carbon Nanotube (SWCNT) and Multiwall Carbon Nanotube (MWCNT). Source: [19].

A negative attribute of CNTs is their tendency to agglomerate when added to a matrix [20]. According to Moniruzzaman and Winey [21], the CNT preparation method, purification, size and orientation in the polymer matrix can lead to "inconsistencies" reported in current literature regarding improvements in nanocomposite performance.

Silica, Ni and Ni/NiO nanoparticles were also investigated in this research. Silica nanopowder is a common filler for nanocomposite materials. Silica is not an effective conductor of heat or electrons, making it an excellent insulator. In contrast, Ni nanoparticles are highly conductive.

C. FOCUS AND APPROACH OF PRESENT STUDY

This research focused on characterizing nanocomposites after exposure to UV light, humidity (in the form of condensation) and salt fog with the goal of identifying the changes in visual appearance, macro and microscopic structural features and quantifying their mechanical and electrical properties. Neat epoxy and nanocomposites consisting of 1% weight CNTs, SiO_2, Ni and Ni/NiO in epoxy resin were fabricated. The samples were exposed to cycles of augmented weather conditions including UV and humidity (in the form of condensation) or salt fog. The maximum treatment time was 246 hours. Vickers hardness measurements were taken and tensile tests were conducted prior to exposure and

periodically throughout exposure. Samples were also analyzed using optical microscopy, electrical resistivity and Fourier Transform Infrared Spectroscopy (FTIR). In addition, neat epoxy and nanocomposites were prepared using CNTs, Ni and Ni/NiO but back with 315L stainless steel shim. After augmented weather exposure, the samples were prepared for Scanning Electron Microscope observation to analyze the stainless steel and epoxy interface.

THIS PAGE INTENTIONALLY LEFT BLANK

II. EXPERIMENTAL METHODS

A. OVERVIEW

This chapter presents the materials, methods and instrumentation utilized to fabricate nanocomposite specimens to expose the samples to augmented weather conditions and to evaluate the changes suffered after exposure. The first section describes the fillers employed, the second explains the protocol used to introduce them in an epoxy matrix, the third offers the specifics of the exposure treatments (UV, temperature and salt fog) and the fourth defines the instruments and conditions used to evaluate the changes suffered by the nanocomposites.

B. NANOFILLERS

The nanofillers selected for the fabrication of nanocomposites were acquired using commercial sources or prepared at the Naval Postgraduate School (NPS) Laboratories. We employed multiwall carbon nanotubes (MWCNT>95% OD x L 6–9 nm x 5 μm, Sigma-Aldrich), silica nanoparticles (nanopowder, 10–20nm Sigma-Aldrich) and nickel nanoparticles (nanopowder, <100nm, Sigma-Aldrich). The fourth filler used, nickel nickel–oxide (Ni/NiO) nanoparticles, was fabricated by heating the Ni nanoparticles mentioned above under oxidizing conditions. Table 1. presents a list of the fillers.

Ni/NiO nanoparticles fabrication. Approximately 350 mg of nickel nanoparticles were spread evenly in the bottom of a sintered alumina ceramic boat (Coors). The ceramic boat was placed in a 2.54 cm (1 inch) diameter quartz tube in a Lindberg Blue M 1200-degree Celsius tubular furnace. The nickel nanoparticles were heated at 200ºC in an air atmosphere for 10 min and kept in the oven until cooled. The temperature and length of the treatment were determined previously by thermogravimetric analysis (TGA). The presence of Ni/NiO after the initial TA and the furnace treatment were confirmed using X-ray diffraction (XRD), and the size of the nanoparticles was confirmed using Scanning Electron Microscopy (SEM).

Table 1. Nanofillers Used.

Filler	Features of interest
SiO2 nanoparticles	Nanometric (10-20 nm), non-electrically conductive filler Density ~ 2.4 g/cm^3 [22]
MWCNT	Nanometric structure (OD x L 6–9 nm x 5 μm), electrical and thermal conductor, low density, high length to diameter ratio Density ~ 2.1 g/cm^3 [23] Conductivity ~ 100 s/cm
Ni nanoparticles	Nanoparticle (<100nm), electric conductor Density ~ 8.9 g/cm^3 [24]
Ni/NiO nanoparticles	Nanoparticle with a conductive core-insulating shell

C. FABRICATION OF EPOXY NANOCOMPOSITES

An epoxy resin commercial kit (EpoFix for metallic backed samples, SpeciFix-20 for non-metallic backed samples, Struers) was used to generate the polymeric matrix of all samples. The basic procedure used to generate the epoxy resin specimen consists of mixing seven parts in volume of resin to one part of curing agent at room a temperature. The initial mixture behaves as a highly viscous liquid, which polymerizes and cures generating a solid after approximately 24 hours. Given that the polymer solidifies in the shape of the container, molds were used for all samples. The first mold used a stiff silicon mat as a base and 5.08 cm by 2.54 cm (2 by 1 inch) glass slides to form molds of various sizes, typically 5.08 cm by 20.32 cm (2 by 8 inches). The glass sides were firmly fixed to the polymer sheet using a thin layer of soft paraffin wax (CAS 8009–03-8, Unilever) and all surfaces were subsequently coated with vacuum grease to facilitate removal of the sample. The second mold used was a flexible silicone mold measuring 5.40 cm by 7.94 cm (2.125 by 3.125 inches). The silicone mold was cleaned with ethanol, dried and coated with vacuum grease prior to pouring the epoxy mixtures. A layout of the preparation method can be seen in Figure 7.

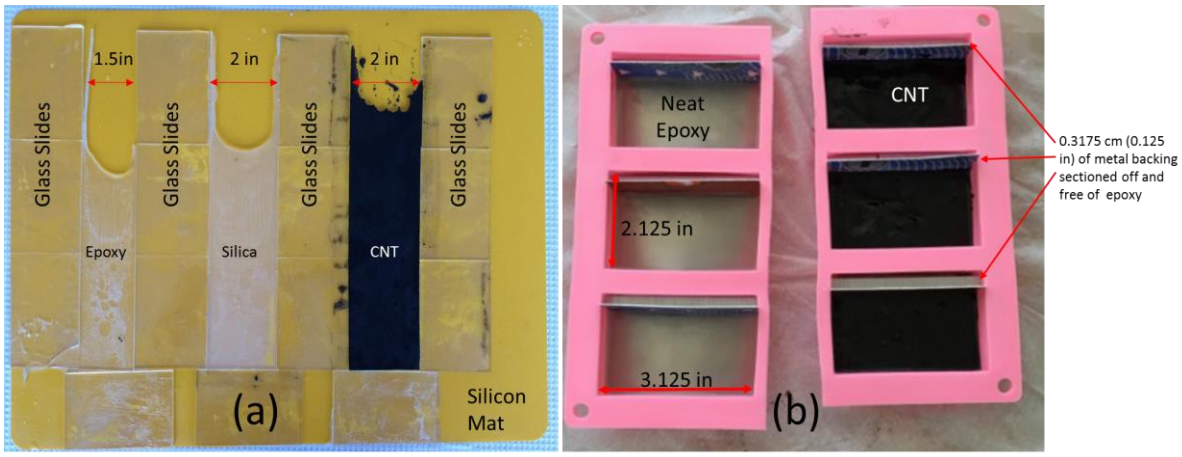

Figure 7. Epoxy Composites Curing (a) on a Silicon Mat and (b) in a Silicon Mold with Metallic Backing.

The nanocomposites were fabricated using the four fillers described in the previous section (SiO2 nanoparticles, MWCNT, Ni and Ni/NiO nanoparticles) and, in order to have baseline data for the epoxy system, a sample was produced with no filler added. The exemplary protocol consisted of adding 7g of curing agent to 35g of epoxy in mixing cup. A thin piece of wood was used to stir the mixture until the components seemed well incorporated and the mix translucent. The mixture was further mixed in a Buehler ULTRAMET 2005 sonic cleaner bath for 5 min. For the neat epoxy samples, the mixture was poured into the molds after sonication. For the nanocomposites, one percent by weight, approximately 0.42g, of nanofiller was measured and added to the resin and curing agent mixture and sonicated for 5 min. The mixture was poured into a mold and allowed to cure for 24 hours. The selection of the 1% loading was decided based on literature research and previous experience with CNT-epoxy composites, since low levels of loading, usually no more than 5% are enough to produce significant changes in properties.

In addition to the neat epoxy and epoxy nanocomposite samples, two sets of four samples were fabricated to contained a partial metallic back in order to study the interfaces between the polymer and the metallic backing after UV and humidity exposure. Each set was exposed to different conditions (one UV-temperature and the other salt fog). The epoxy nanocomposite-metallic back specimens were created using the same techniques but were poured on top of a pretreated sheet of metallic shim 316L

stainless steel trimmed to 7.62 cm by 27.94 cm (3 by 11 inches). The stainless steel shim pretreatment consisted of applying diamond polish (POL) to the surface to create a porous substrate to bond with the epoxy. Silicone molds were used again and the epoxy mixtures were poured directly onto the stainless steel surface and allowed to cure for 24 hours. The resulting sample thickness ranged from 2–4 mm. A summary of the samples generated can be found in Table 2.

Table 2. Samples Generated.

Sample	Treatment	Characterization
Epoxy – Neat	3 QUV Cycles	Optical Microscope Hardness Tensile Test Electrical Conductivity FTIR
Epoxy – MWCNT	3 QUV Cycles	Optical Microscope Hardness Tensile Test Electrical Conductivity FTIR
Epoxy – SiO2	3 QUV Cycles	Hardness Tensile Test
Epoxy – Ni	3 QUV Cycles	Optical Microscope Hardness Tensile Test Electrical Conductivity FTIR
Epoxy - NiO	3 QUV Cycles	Optical Microscope Hardness Tensile Test Electrical Conductivity FTIR
Epoxy – Neat, metallic backing	3 QUC Cycles 3 Salt Fog Cycles	SEM
Epoxy – MWCNT, metallic backing	3 QUC Cycles 3 Salt Fog Cycles	SEM
Epoxy – Ni, metallic backing	3 QUC Cycles 3 Salt Fog Cycles	SEM
Epoxy – NiO, metallic backing	3 QUC Cycles 3 Salt Fog Cycles	SEM

Table of samples generated, treatment type and characterization method.

In order to facilitate hardness readings as well as eventual SEM analysis, the samples consisting of neat epoxy and Ni/NiO, Ni, and CNT nanocomposites, were polished. The samples were sanded initially by hand using 120, 200, 400 and 600 grit sandpaper until they had a smooth surface. The process was then modified to using a rotary fabric head polisher. Each sample was polished using 3µm and 1µm Alumina Oxide (Al_2O_3). 3 µm Al_2O_3 was applied to surface while using the polishing head for ten minutes. The sample was checked in the optical microscope to ensure any scratches were smaller than 10 µm in length. The process was repeated using 1 µm Al_2O_3 and the samples were checked for scratches less than 5 µm in length.

D. ARTIFICIAL WEATHER EXPOSURE

An accelerated weather chamber by QUV was used to simulate natural sunlight and humidity with UVA-340 lamps and a condensation chamber. According to Q-Lab, the exposure cycle must run with moisture to match natural environments. In addition, Q-Lab reported that UVA-340 lamps, does not cause any unnatural yellowing [25]. A salt fog chamber was also used for metallic backed samples to simulate a corrosive sea environment.

1. ACCELERATED WEATHER CHAMBER

The samples were exposed to a QUV Accelerated Weathering Tester. Utilizing fluorescent lamps and a water tray, the QUV simulates sunlight and dew by alternating between cycles of UV light and moisture at set temperatures and irradiance levels. A schematic of the QUV is provided in Figure 8. A UVA-340 lamp was used, which simulates sunlight from 295 to 365 nm (Figure 9) [25]. All samples were secured in standard flat panel holder part of the QUV system, as seen in Figure 10. Only the portion of the samples that was exposed to the UVA lights were subsequently analyzed using the microhardness reader and tensile tester. The samples were exposed to 64–96 hour cycles, removed and a portion was cut for hardness testing. The remaining samples were returned to the QUV until a total of 246 hours of exposure was completed.

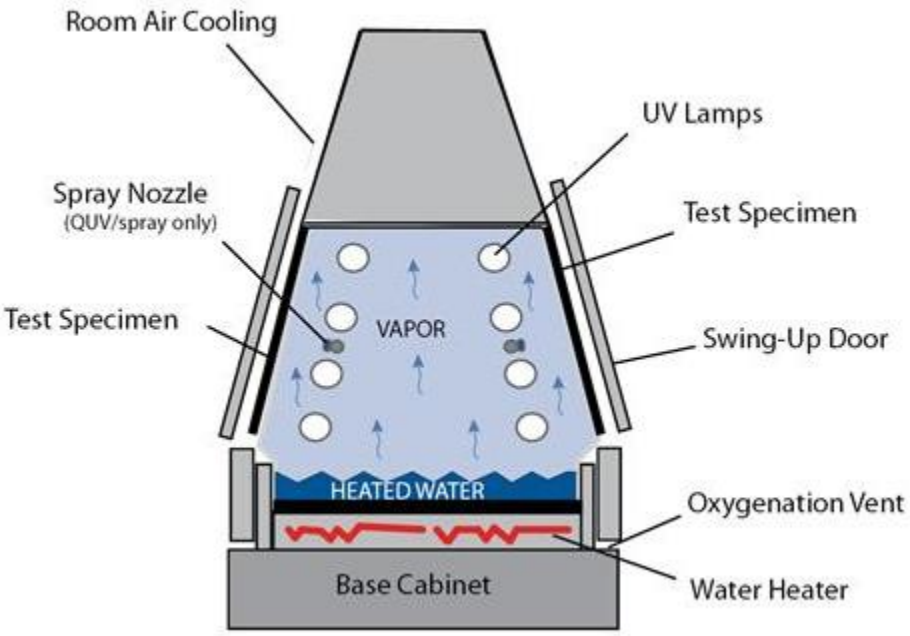

Figure 8. Schematic of QUV Accelerated Weather with Water Tray Tester. Source: [25].

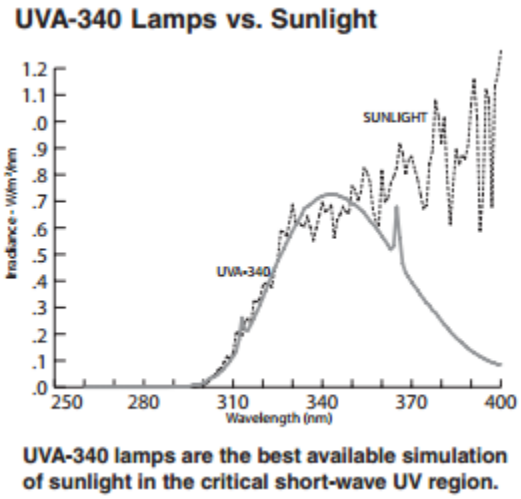

Figure 9. UVA 340 Lamps versus Sunlight. Source: [25].

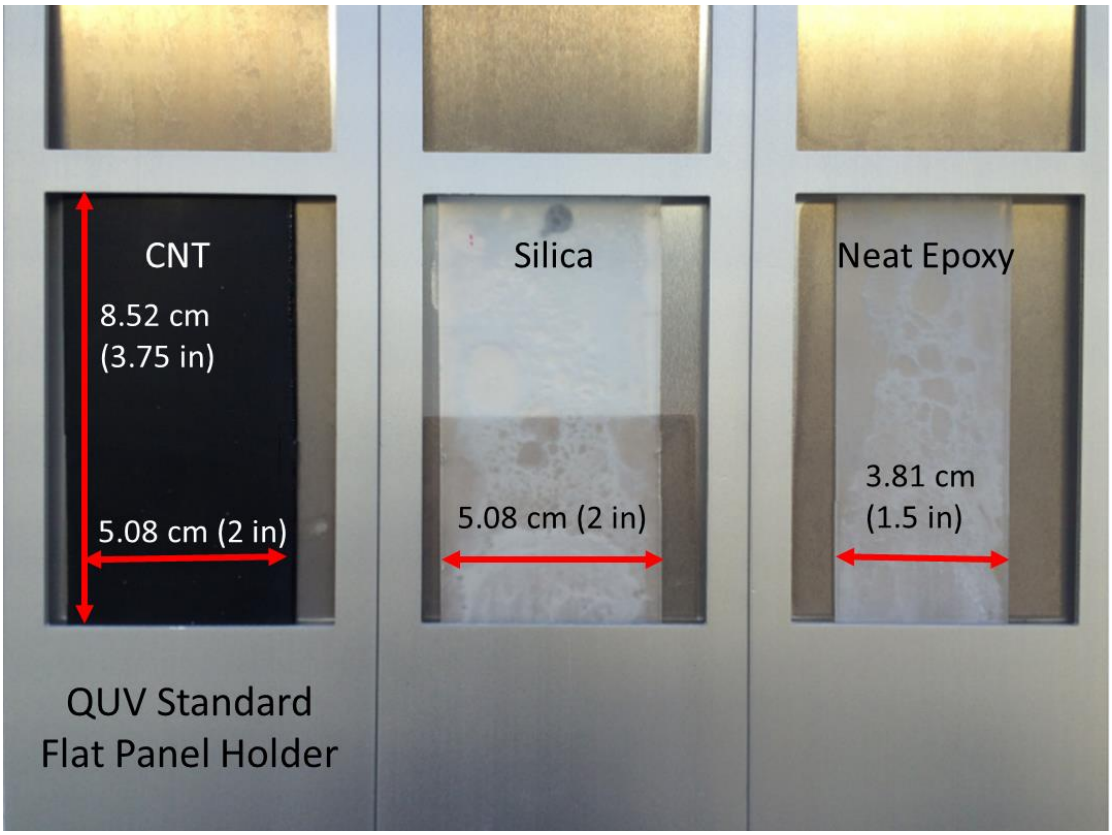

Figure 10. CNT, SiO_2 and Neat Epoxy Samples Mounted in QUV Standard Flat Panel Holder Prior to Initial Exposure.

2. SALT FOG CHAMBER

The metallic backed samples were treated in a salt spray test chamber. The salt spray test chamber is an Associated Environmental Systems MX series. The samples were exposed concurrently with the QUV metallic backed samples. At the end of each cycle the chamber was switched off, the samples were removed and a portion was cut for further analysis before returning the sample to the chamber. The Salt Fog chamber operating with metallic backed neat epoxy, CNT, Ni and Ni/NiO samples are shown in Figure 11.

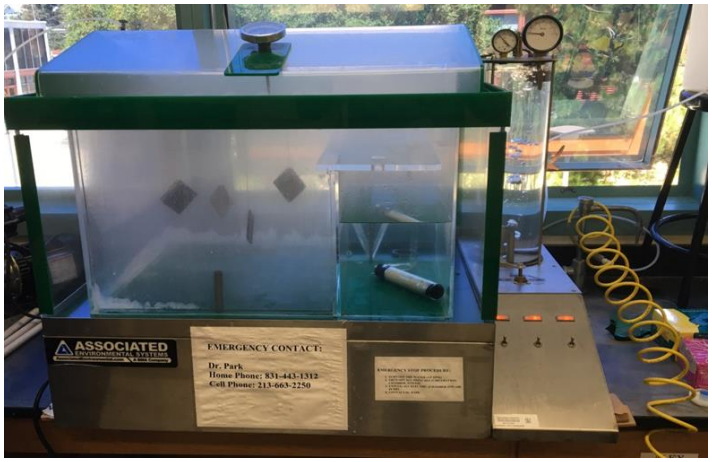

Figure 11. Metallic Backed Neat Epoxy, CNT, Ni and Ni/NiO Samples Suspended in Salt Spray Test Chamber During Operation.

E. SAMPLES CHARACTERIZATION AND TESTING

A variety of techniques were used to analyze and characterize the samples prior to and post exposure in the QUV and salt fog chambers. Optical microscopy was performed to check surface preparation prior to exposure and condition of the surface after exposure. Vickers hardness measurements were taken to compare before and after exposure and amongst samples. Tensile tests were performed to determine the effect of UV light and humidity on the samples young modulus, yield and tensile strength. Electrical resistivity was measured in order to determine the effect of varying levels of conductivity in the samples on the performance of the nanocomposites. FTIR was performed to determine modification on the chemical groups present in the samples. Finally, SEM images were taken on metallic backed samples to analyze the impact of cycling weather conditions on the epoxy-metallic interfaces.

1. OPTICAL MICROSCOPE

A Nikon Epiphot 200 Inverted Metallurgical Microscope was used to evaluate the samples surface characteristics. The microscope was used during the polishing process to verify the absence of scratches that would hinder further study. Also, the optical microscope was used to study the surface of the samples after exposure for signs of charring and cracking.

2. HARDNESS

A Struers DuraScan-70, low load hardness tester was used to determine hardness before the samples were treated and after each 96 hours of exposure in the QUV. Vickers hardness measurements were taken in accordance with ASTM E384. Measurements were done in series with HV 0.1 and HV 0.025 loads.

3. TENSILE TEST

Post each cycle of exposure in the QUV, three samples with dimensions 1.5 x 5 cm were cut from the samples using Struers SECOTOM-10 tabletop cut-off machine at 0.025mm/min (Figure 12). The samples were then machined to a uniform size using a flat end mill with mill vise jaws. A ball end mill was used to cut a smaller cross section in the centerline of the sample (to assure that necking and fracture will occur in that zones while) while it was held with mill vise jaws.

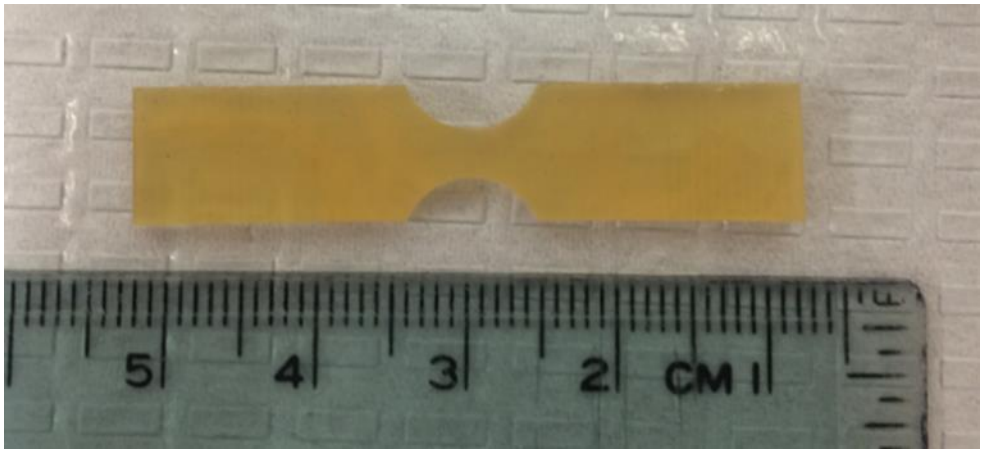

Figure 12. 1.5 cm x 5 cm Tensile Test Specimen after Exposure to UV and Humidity prior to Tensile Test.

An Instron model 4507 was used to conduct tensile tests for neat, CNT, Ni and Ni/NiO epoxy samples before and after each type of exposure. The samples were cut to a traditional, flat specimen shape with a 5.77 mm (0.2271654 in) gauge length. The samples were mounted using a wedge-type grip. The test was conducted at 0.1 mm/in.

The data was used to determine changes in modulus of elasticity and ultimate tensile strength after exposure and amongst the four types of samples.

4. ELECTRICAL RESISTANCE AND RESISTIVITY

Electrical resistivity was measured for the neat epoxy, CNT, Ni and Ni/NIO samples as prepared and after each cycle of exposure to determine if electrical conductivity was altered after exposure. A 4-point probe meter (Lucas Labs Pro4, PRO4-4400) collected resistivity, which was converted into electrical conductivity (S/m). The data was collected using a Lucas Signatone Corporation Pro4 software.

5. FOURIER TRANSFORM INFRARED SPECTROSCOPY

Fourier Transform Infrared Spectroscopy (FTIR) was employed to determine the presence of various chemical groups through periods of hydration and UV exposure. FTIR was conducted by researchers at Universidad Nacional de Colombia. The samples analyzed included the neat epoxy, the CNT, Ni and, Ni/NiO nanocomposite samples, as prepared and after the first and second cycle of exposure. FTIR profiles were obtained using a universal sampling accessory PIKE MIRacle attached to a FTIR Nicolet iS 10 spectrometer (Thermo Fisher Scientific). The samples were scanned with a continuous wavelength range of 700 to 3900 cm^{-1}. Spectral intensity and wavelength were provided and subsequently graphed for analysis.

6. SCANNING ELECTRON MICROSCOPE

A Zeiss 40 NEON field emission scanning electron microscope (SEM) was used to analyze the effects of exposure on the metallic backed epoxy samples. A Cressington 280HR high-resolution sputter coater was used to coat CNT and Ni/NiO samples (with and without exposure in the QUV) with a layer of Pt-20Pd. The samples were placed in a Pelco 2251 vacuum desiccator for 24 hours prior to observation in the SEM. The samples were observed using 20 KV and 1.33 x 10–^{6} mA current at a 5 mm working distance.

Post exposure in the QUV, the metallic backed samples were prepared for a cross sectional analysis in the SEM. Given the fragility of the metallic-epoxy interface due to the geometry that samples acquired after being heated, the samples were cold mounted.

The samples were cut to 1 x 7.62cm (0.3937 x 3 in) and mounted in plain, Epofix-20 epoxy according to the manufacturer's recommendations (Figure 13).

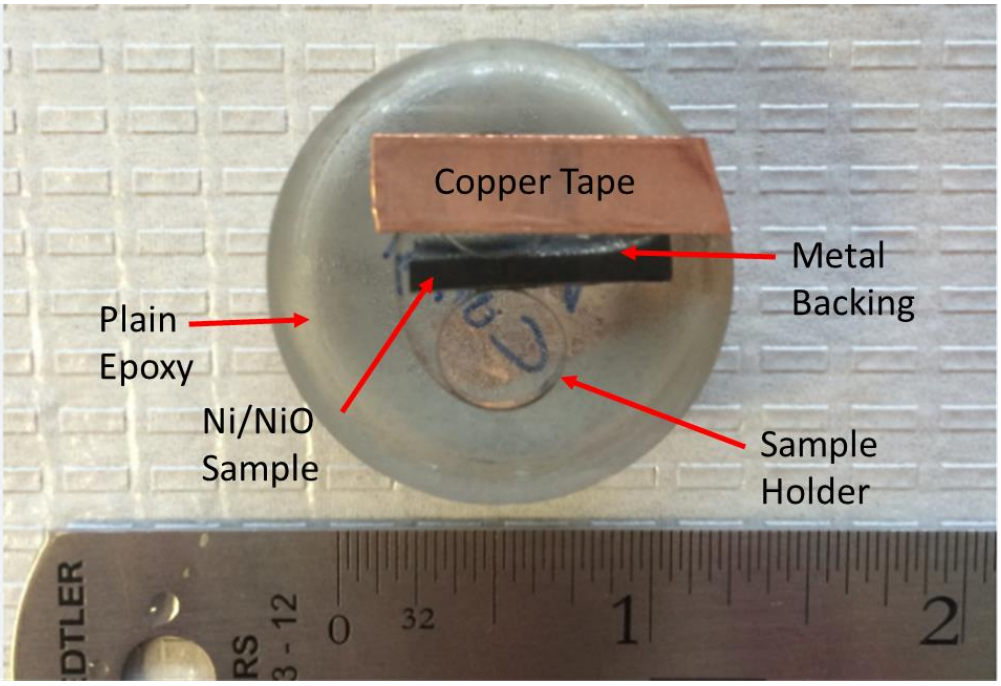

Figure 13. Cold-Mounted Ni/NiO Metallic Backed Sample Prepared for SEM Analysis.

After 24 hours of curing time, the samples were cut in order to remove the excess weathered epoxy and expose metallic interface. A Buehler ISOMET low speed saw with a Buehler Diamond cut-off blade was used initially to cut samples. Since the low speed saw proved to take long time (approximately 10 hours) to section the specimens, the remaining samples were cut with the Struers SECOTOM-10 tabletop cut-off machine at 0.025mm/min (0.00098425197in/min).

Six samples (unweathered CNT and Ni/NiO and weathered plain epoxy, CNT, Ni, and Ni/NIO) were mounted and sanded using the Buehler ECOMET 4 grinder/polisher with the Buehler AUTOMET 2 power head with 320, 800, 1200, 2000 and 4000 SiC-paper. The samples were cleaned with ethyl alcohol and polished in the Buehler VibroMet 2 Vibratory Polisher at 90% amplitude. A Buehler 12 in. microcloth was used with distilled water and the samples were mounted in a Buehler specimen loader with no

added weight. The samples were first polished using 1 μm Al_2O_3. After 24 hours, the samples were removed and individually cleaned for 10 min using ethyl alcohol in a Buehler ULTRAMET 2005 sonic cleaner. The samples were checked in the optical microscope. After cleaning the VibroMet, the samples put back in for 24 hours using 0.05 μm Al_2O_3, cleaned and checked for scratches in the optical microscope.

III. RESULTS AND DISCUSSION: EPOXY WITH NANOFILLERS

A. NANOFILLERS

All the filler particulates SiO_2, CNT, Ni and Ni/NiO were analyzed by SEM prior to their inclusion in the epoxy resin. The images acquired show that the structure of all nanofillers, powder and tubes, have at least one dimension smaller than 100 nm. The SiO_2 nanopowder was composed of agglomerated irregular shaped particles of sizes in the range 10–70 nm. With the case of the CNT, the average diameter of the tubes was determined to be approximately 10 nm-30 nm while the length of the tubes exceeded the micron range (10 μm). The Ni and Ni/NiO nanopowders were both spherical in shape but the Ni/NiO seem to be forming agglomerates. The Ni and Ni/NiO were similar in size, with an average of 50 nm diameter. Images of these samples are seen in Figure 14, Figure 15, Figure 16, and Figure 17.

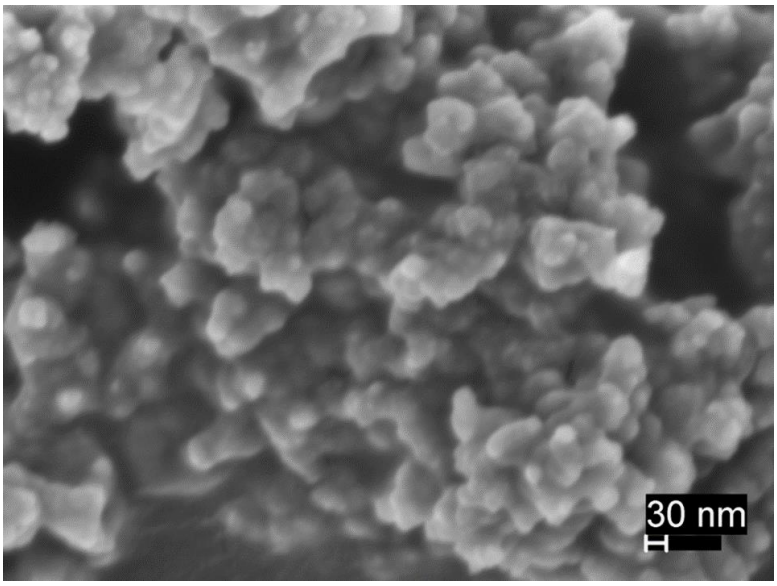

Figure 14. SEM Image of as Received SiO_2 Nanoparticles Showing Particles on the Nanoscale.

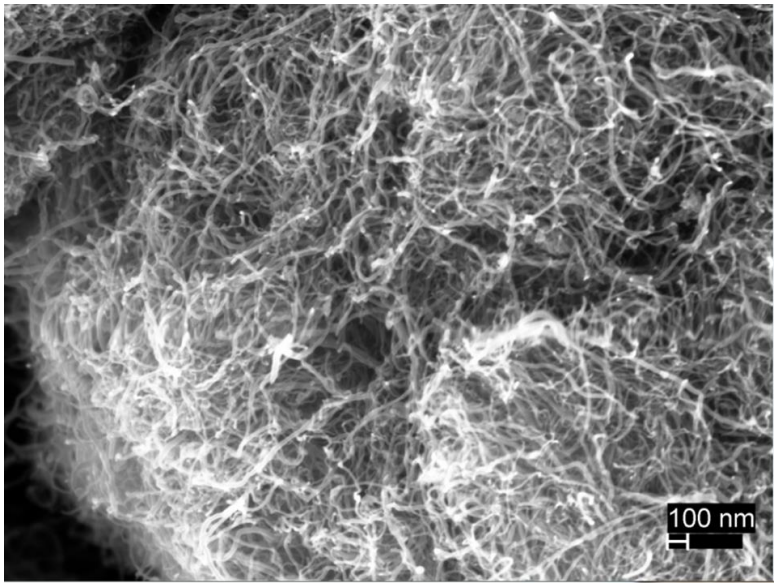

Figure 15. SEM Image of Tangled MWCNTs Showing a Diameter on the Nanoscale with a Length Longer than 100 nm.

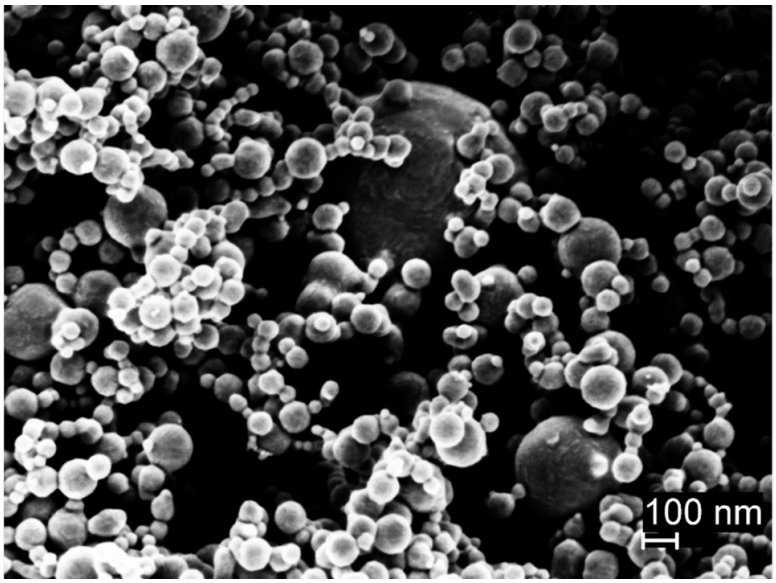

Figure 16. SEM Image of Nickel Globules Under 100 nm.

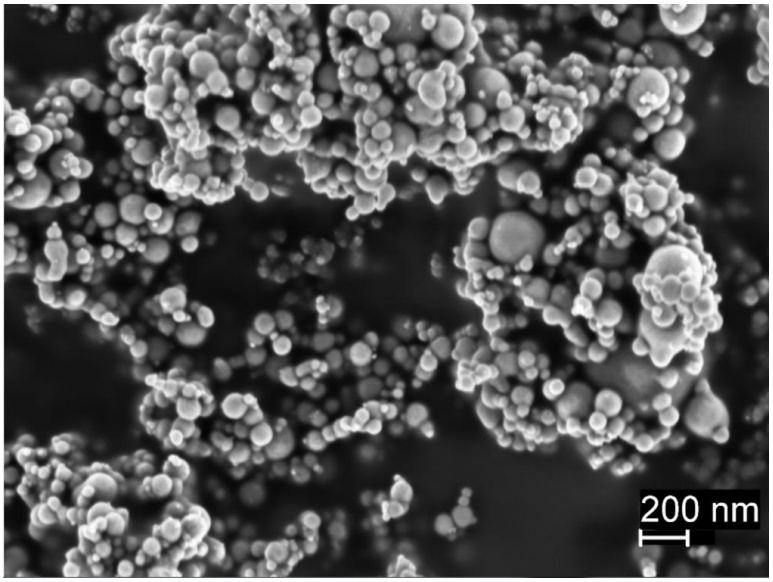

Figure 17. SEM image of Ni/NiO Globules on the Nanoscale.

B. EPOXY AND NANOFILLER COMPOSITES

This section describes the results of the neat epoxy and SiO_2, CNT, Ni and Ni/NiO composites after UV and humidity exposure. The results show dramatic changes in the color some of samples and well as the surface structure. Hardness and tensile test data showed a trend after exposure while the sheet resistance showed little change. Finally, the FTIR results showed significant chemical changes in the samples.

1. VISUAL RESULTS

The samples were examined prior to and post artificial weather exposure. An image of neat epoxy, CNT and SiO_2 samples post tensile test is provided in Figure 18. The neat epoxy and silica samples experienced similar visual changes. Both epoxies changed from transparent solids to opaque tinged yellow, the color became darker after each cycle. The CNT samples exhibited a minor color change from black to an opaque dark green.

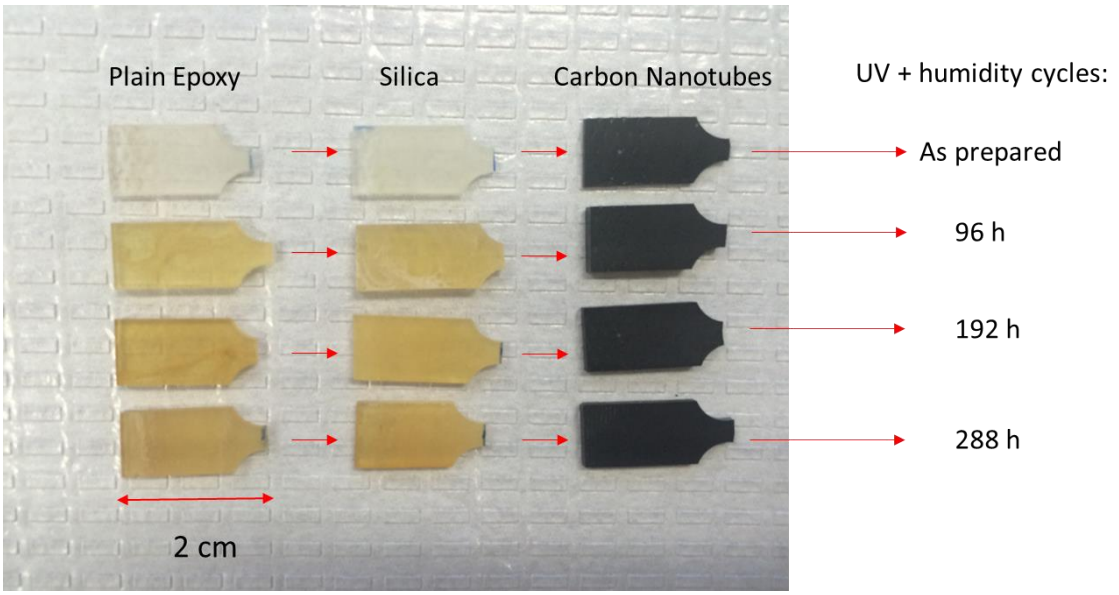

Figure 18. Color Change and Surface Degradation of Neat Epoxy, SiO2 and CNT Samples (Image Taken after Tensile Test Conducted).

Figure 19 shows a Silica sample after three cycles of exposure. The fully exposed center shows the dark yellow color, while the ends, which were partially and fully covered by the QUV standard sample, holder show little to no change in color.

Figure 19. Color Change and Exposure Comparisons for $Si0_2$ Sample after Partial Exposure, 3 Cycles of Exposure and No Exposure to UV Light.

Images of the neat epoxy and epoxy - CNT, Ni and Ni/NiO composites, after machined into tensile test specimens are seen in Figure 20. For each set of conditions, we fabricated 3 tensile specimens (not shown), allowing us to repeat the measurements and have higher confidence in the trends observed. The neat epoxy experienced the most dramatic visual change. Similar to the prior set of neat epoxy samples, after the first cycle in the QUV lasting 54 hours, the neat epoxy was tinged yellow. The Ni and Ni/NiO samples also exhibited an increasingly yellow surface as QUV exposure increased. In contrast to the plain epoxy, the yellow surface appears patchy and inconsistent. In comparison, the CNT samples seem to be less impacted but still present surface scaling (yellow deposits).

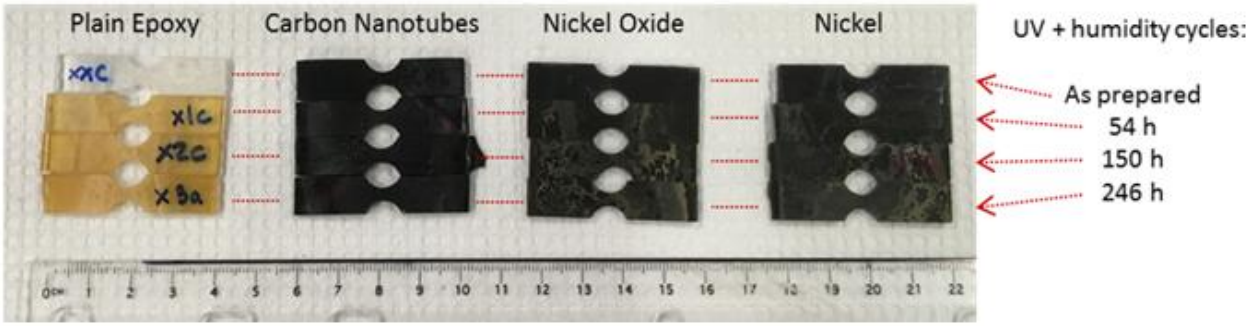

Figure 20. Color Change and Surface Degradation of Neat Epoxy, CNT, Ni and NiO Sample after Exposure to UV and Humidity.

2. OBSERVATIONS FROM OPTICAL MICROSCOPE

Figure 21 depicts optical micrographs of the neat epoxy and the epoxy with CNT, Ni and Ni/NiO samples before QUV exposure and after 246 hours of exposure. The plain epoxy specimen presents a high density of linear microcracks roughly 100 µm in length across the sample surface. The Ni and Ni/NiO samples exhibited an increased amount of microcracks when compared to the epoxy, the cracks are curved or follow irregular paths and interact with each other, they are shorter in length than the ones observed in the bare epoxy. In comparison, the MWCNT samples displayed the fewest linear microcracks, although the cracks seem to propagate in straight paths and do not seem to be interconnected, most are in the 100 µm length.

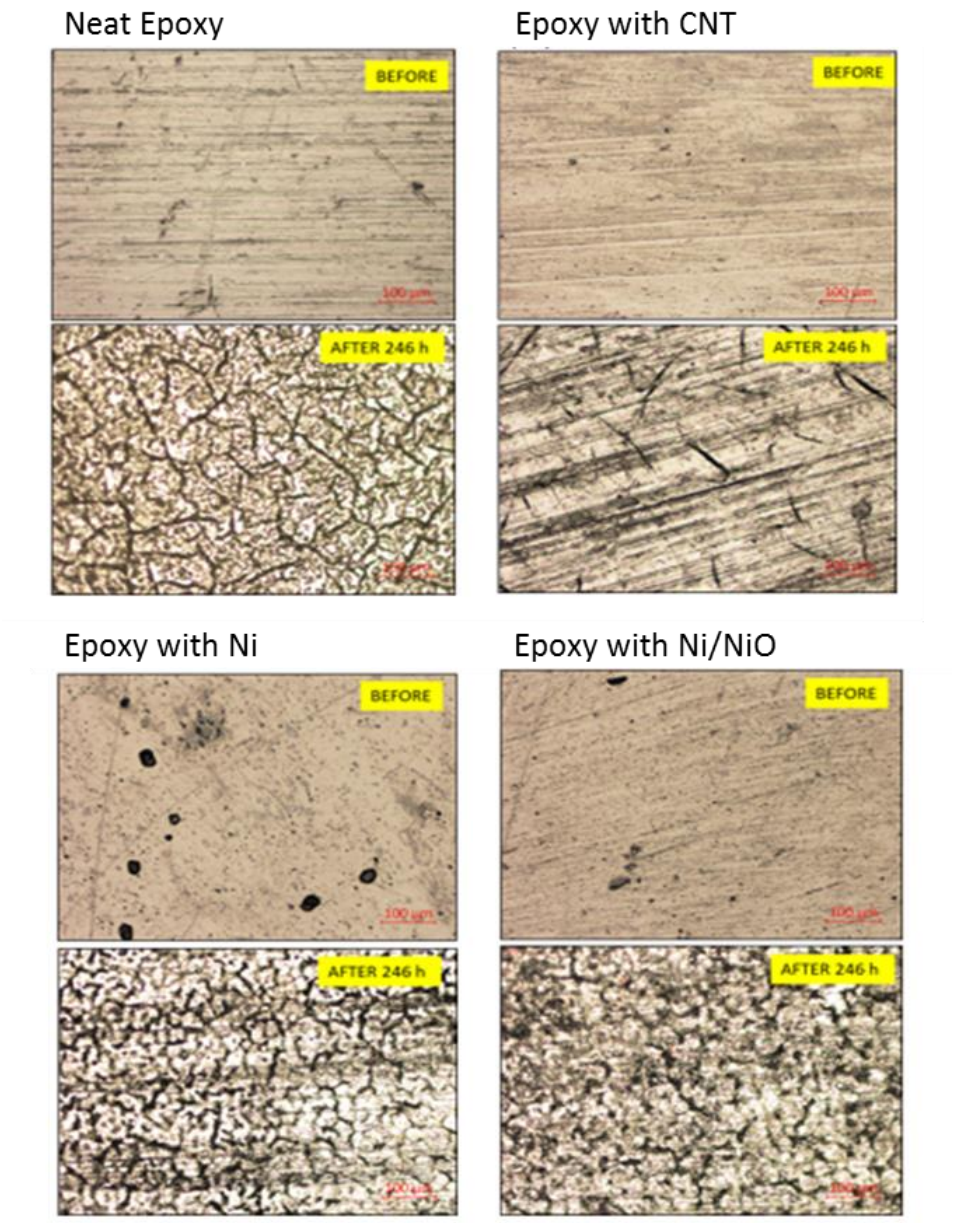

Figure 21. Optical Microscope Images of Neat Epoxy, CNT, Ni and Ni/NiO Samples before and after UV and Humidity Exposure.

3. HARDNESS VALUES

Micro-hardness testing was conducted for each sample after each cycle in order to track the effects of exposure on the samples. The neat epoxy, CNT, and Ni/NiO samples each showed a similar trend throughout the three cycles of exposure, as seen in Figure 22.

Noticeable among all samples is a steady increase in hardness after each cycle; however, the hardness data became more dispersed (higher variability) after exposure. The CNT and Ni/NiO sampled had the lowest standard deviation of 0.2 and 0.3, respectively, after the first cycle, which increased to 1.27 and 1.16 after the third cycle (Table 3). It is worth noting that the neat epoxy had an initial hardness of 15.97 HV, which was 11.4% greater than that of the CNT. This is likely a result of uneven dispersion of the CNTs in the epoxy and the relatively low loading of 1% CNT in composite. In comparison, after the third cycle, the hardness of the CNT increased by 37.2% to 19.68 HV while the neat epoxy only increased by 17.8% to 18.82 HV. Overall, the Ni nanocomposite had the greatest increase in hardness from 13.96 HV to 21.16 HV (a 51.6 % increase). The Ni nanocomposite also had the largest initial standard deviation of 1.5, which eventually decreased to 0.9 after third cycle. The CNT and Ni/NiO samples were the only samples to experience a decrease in hardness after cycles two and one respectively. This loss in hardness might indicate the period when the samples were more affected by the condensation cycle of exposure versus the UV cycle, indicating hydration and loss of hardness.

Table 3. Hardness Values for Neat Epoxy and CNT, Ni and Ni/NiO Nanocomposites.

		Neat Epoxy	CNT	Ni	Ni/NiO
As Prepared	Average HV	15.97	14.34	13.94	14.67
	Standard Deviation	0.5	0.2	1.5	0.3
Cycle 1	Average HV	16.70	17.4	16.93	14.44
	Standard Deviation	1.0	0.9	1.1	0.8
Cycle 2	Average HV	18.51	16.24	17.41	17.71
	Standard Deviation	0.8	0.9	0.9	1.2
Cycle 3	Average HV	18.82	19.68	21.16	19.96
	Standard Deviation	1.4	1.3	0.9	1.2

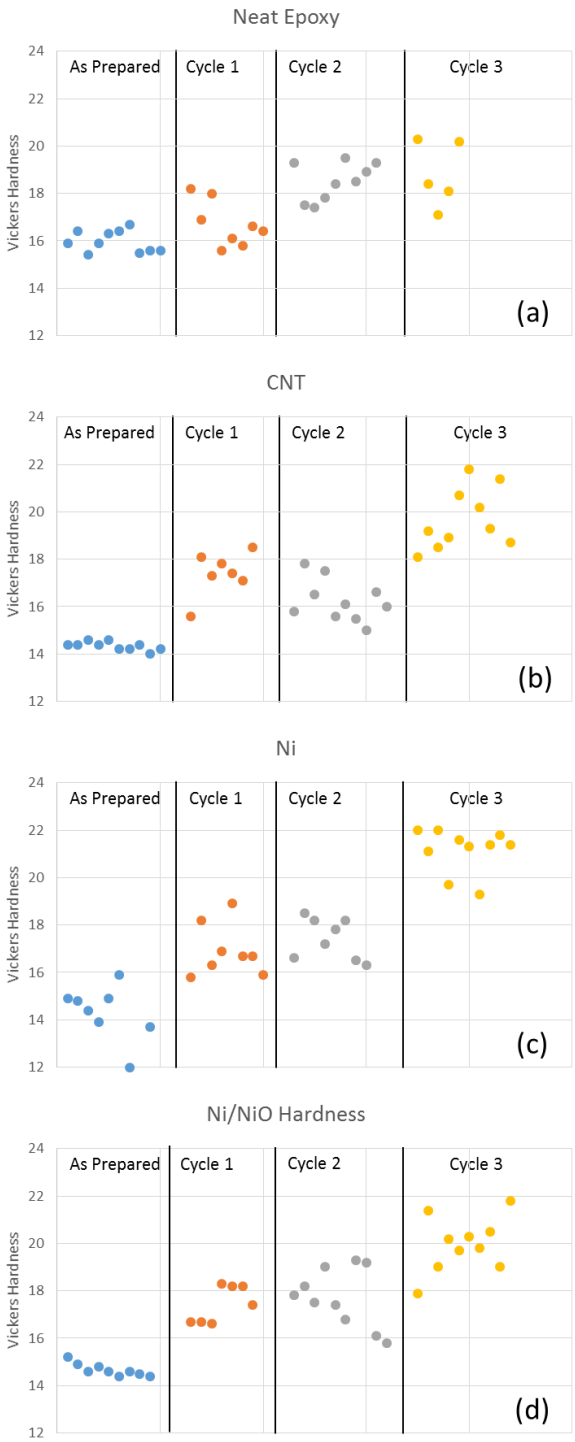

Figure 22. Vickers Hardness for (a) Neat Epoxy, (b) CNT, (c) Ni, and (d) Ni/NiO before and after UV and Humidity Exposure.

It is easier to compare hardness values among the ‘as prepared’ epoxy resin and epoxy-filler samples than the samples following weather exposure. As seen in Figure 23, (a), the neat epoxy has the highest hardness averaging 15.97. The CNT and Ni/NiO samples are relatively comparable, averaging 14.34 and 14.67, respectively. Three outliers in the Ni data prevent further conclusions to be made regarding the hardness as prepared.

As the samples are exposed to UV light and humidity, the hardness data presents a higher standard deviation (variability) and becomes difficult to compare individual values. What is clear is that, in general, the hardness increased with each exposure. The CNT sample hardness decreases after Cycle 2 but reaches a maximum after the third cycle. After the third cycle, the Ni sample has the highest hardness, 21.16 (and lowest standard deviation). Comparison of the hardness data among the epoxy and epoxy-filler samples showing each measurement, in the order that values were taken, can be found in Figure 23. It is worth mentioning that each point was validated by optical microscopy observation of the indents to assure that the values were not caused by samples surface pores, scratches or other defects.

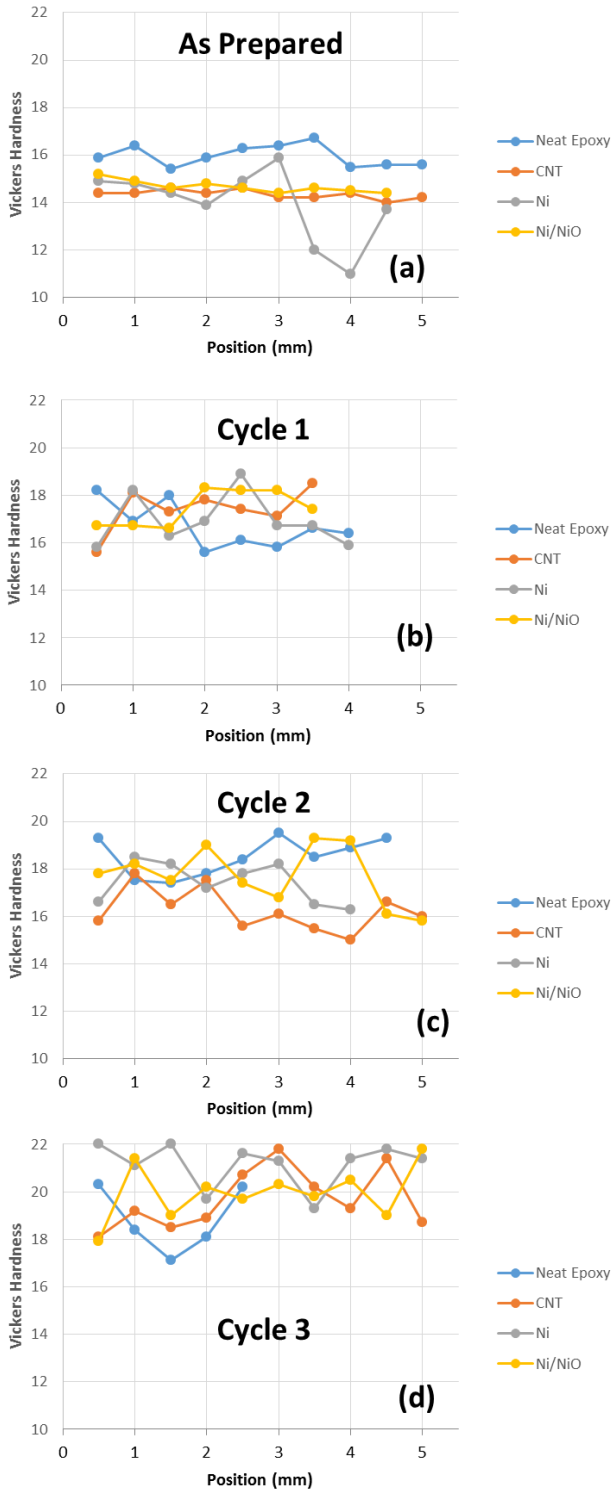

Figure 23. Combined Vickers Hardness for (a) As Prepared, (b) Cycle 1, (c) Cycle 2 and (d) Cycle 3.

It is important to note that only 50% of the data points were usable after cycle 3 for the neat epoxy. The surface became increasingly covered in cracks and anomalies, which obscured the data, making it impossible to calculate accurate hardness values. An example of this can be seen in Figure 24.

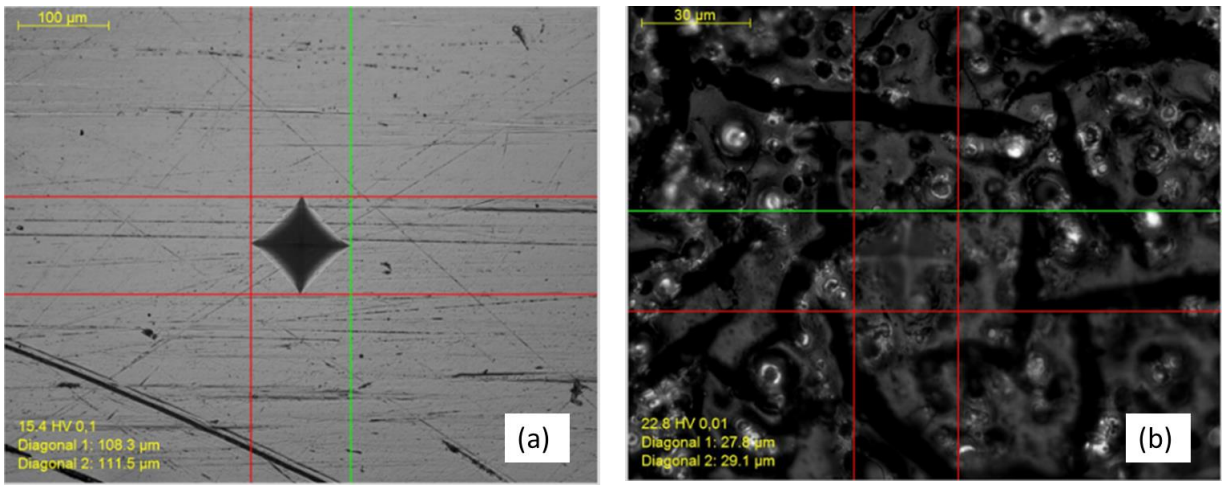

Figure 24. Hardness images of Neat Epoxy (a) as prepared showing no surface anomalies and (b) after Cycle 3 showing anomalies.

4. TENSILE TEST DATA

Tensile tests were conducted for first set of neat epoxy, the epoxy-CNT and epoxy-Silica samples and for the second set of neat epoxy, epoxy-CNT, epoxy-Ni and epoxy-Ni/NiO samples. The information gathered from the first set was used to set the protocols for four samples in the second set. The ultimate tensile strength (UTS) and Young's Modulus were calculated from the tensile test data. The Young's Modulus was determined from the first slope of the stress strain graph. The ultimate tensile strength determined was the maximum stress in the stress vs strain curves, exhibited by the sample before failure. Toughness was determined by evaluating the area under the entire curve. Noticeable in each graph is a plateau observed in the stress values once the yield strength has been reached.

Tensile test data for all samples after each cycle was graphed and is presented in Figure 25, Figure 26, Figure 27, and Figure 28. The ultimate tensile strength of the neat

epoxy initially declined from 85.7 MPa to 69.40 MPa and remained consistent after one and two cycles of UV and humidity exposure. After the final cycle, the ultimate tensile strength increases again to 82.81 MPa. Comparing the toughness after one and two cycles, the toughness appears to decrease slightly after cycle two and the strain is the greatest after cycles one and three. This may indicate water absorption after cycle one creating a more elastic material.

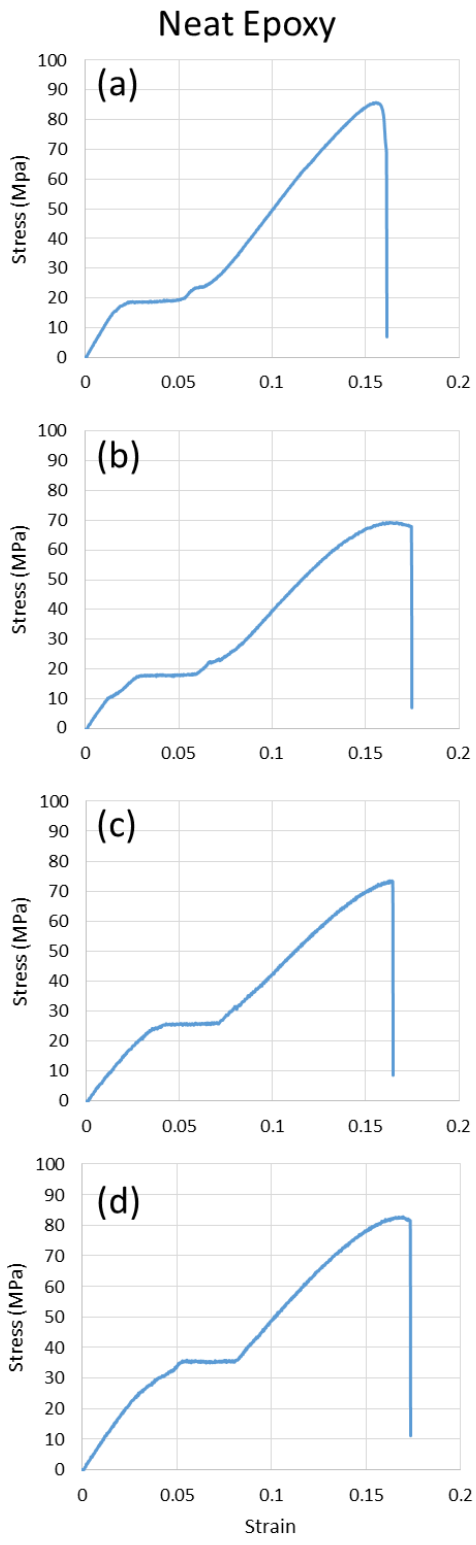

Figure 25. Stress – Strain Graphs of Neat Epoxy (a) as prepared, after (b) Cycle 1, (c) Cycle 2, (d) Cycle 3.

The CNT tensile tests showed the most dramatic response to exposure to UV and humidity. Toughness, strain and ultimate tensile strength all steadily decrease after each cycle of exposure (Figure 26). Initially, the CNT sample had an ultimate tensile strength of 76.55 MPa but this decreased by 46.4 % to 41.02 MPa after the first cycle and 75.9 % to 18.42 MPa after the third cycle. In contrast, the yield strength increased after the first cycle from 23.80 MPa to 15.81 MPa. After the third cycle the yield strength decreases to 8.51 MPa, which is an overall decrease of 46.2%, significantly less than the decrease in ultimate strength of 75.6%. It is worth noting that the CNT samples suffered brittle fractures while attempting to set up the tensile test machine, rendering some samples after cycle two and cycle three unusable. The shape of the CNT stress strain graph also drastically changes after the first cycle. The as prepared curve is relatively ductile while the curves after each cycle of exposure are clearly brittle. The decrease in toughness and strain indicate that the CNT samples were more affected by UV than the humidity of the cycles. The samples were less likely than the neat epoxy to swell and absorb water.

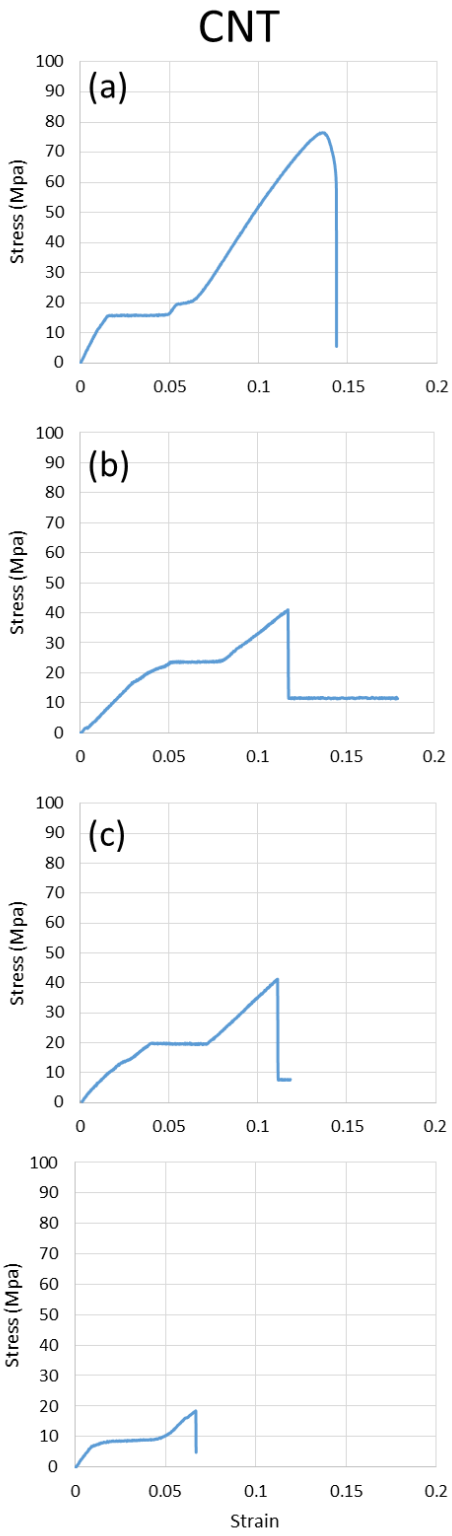

Figure 26. Stress – Strain Graphs of CNT (a) as prepared, (b) Cycle 1, (c) Cycle 2, (d) Cycle 3.

The Ni sample had a more varied response to UV and humidity exposure compared to CNT (Figure 27). After one cycle of exposure, the strain and toughness of the sample increases while the ultimate tensile strength remains the same. This may indicate hydration and swelling (also observed during visual examination) of the sample. After cycle two, the ultimate tensile strength, strain and toughness drastically decrease. As prepared and after cycle one the ultimate tensile strength was 80.53 MPa and 78.69 MPa respectively. After the second cycle, the ultimate tensile strength decreased by 26.0% to 59.58 MPa. The curve for the second cycle sample appears to be more brittle in nature compare to the as prepared and first cycle samples. This trend is also apparent in the third cycle. This indicates that the sample was dry, dehydrated and lost ductility. After the third cycle, it appears that the sample may have rehydrated and slightly increased the strain and toughness of the sample. In addition, the ultimate tensile strength increased to 66.4 MPa from cycle two to cycle three but this is still an overall loss of 17.6% from the as prepared measurement. In addition, the yield strength decreased from 16.21 MPa to 10.08 MPa after the course of three cycles of exposure.

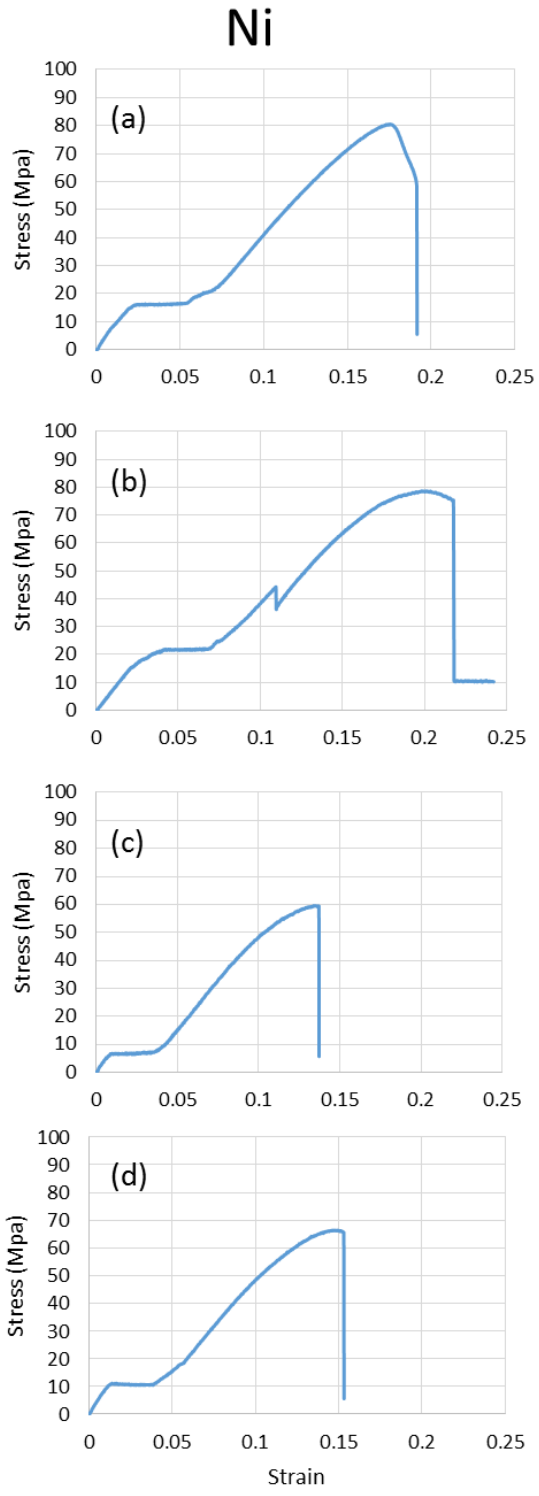

Figure 27. Stress – Strain Graphs of Ni (a) as prepared, (b) Cycle 1, (c) Cycle 2, (d) Cycle 3.

The Ni/NiO samples showed the most dramatic sign of hydration after two cycles of UV and humidity exposure (Figure 28). After one cycle, the ultimate tensile strength decreased slightly but the strain increased which indicates hydration. Initially, the as prepared sample had an ultimate tensile strength of 74.38 MPa, which decreased to 70.28 MPa after one cycle of exposure. After the second cycle, the ultimate tensile strength, strain and toughness increases. The ultimate tensile strength increased by 15.5% from the as prepared sample to 85.9 MPa. In addition, the yield strength increases dramatically from 13.25 MPa to 27.33 MPa, an increase of 106.3% over two cycles. This indicates more hydration of the sample and ductility. After the third cycle, the strain and toughness decreased indicating the sample become dry and losing ductility. In addition, the shape of the curve appears to be the most indicative of a brittle sample compared to the previous samples. The ultimate tensile strength also decreases to 68.22 MPa, an overall loss of 8.3%. Finally, the yield strength decrease to 14.1 MPa, which is still marginally larger than the as prepared sample.

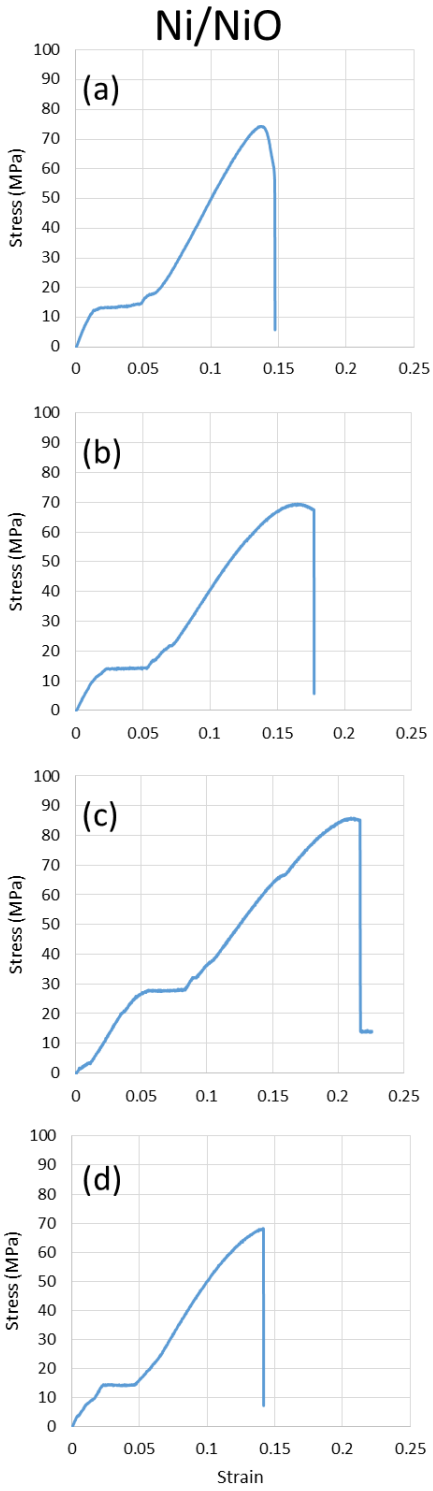

Figure 28. Stress – Strain Graphs of Ni/NiO (a) as prepared, (b) Cycle 1, (c) Cycle 2, (d) Cycle 3.

The UTS of the samples was averaged (3 specimens were made for each condition) and graphed in Figure 29. The "as prepared" samples had similar UTS ranging from 72.9 MPa (neat epoxy) to 77.5 MPa (Ni/NiO). The Neat epoxy and Ni samples' UTS remained relatively consistent after exposure. After Cycle 2, The Ni/NiO sample had an increase in UTS from 77.5 MPa (as prepared) to 83.75 MPa, but decreased after cycle 3 to 69.2 MPa. The UTS of the CNT sample decreased dramatically after each exposure cycle. It decreased by 51.6% after just one cycle. After the second cycle, the UTS increased slightly but again decreased after cycle 3 to 18.4 MPa. (Figure 29).

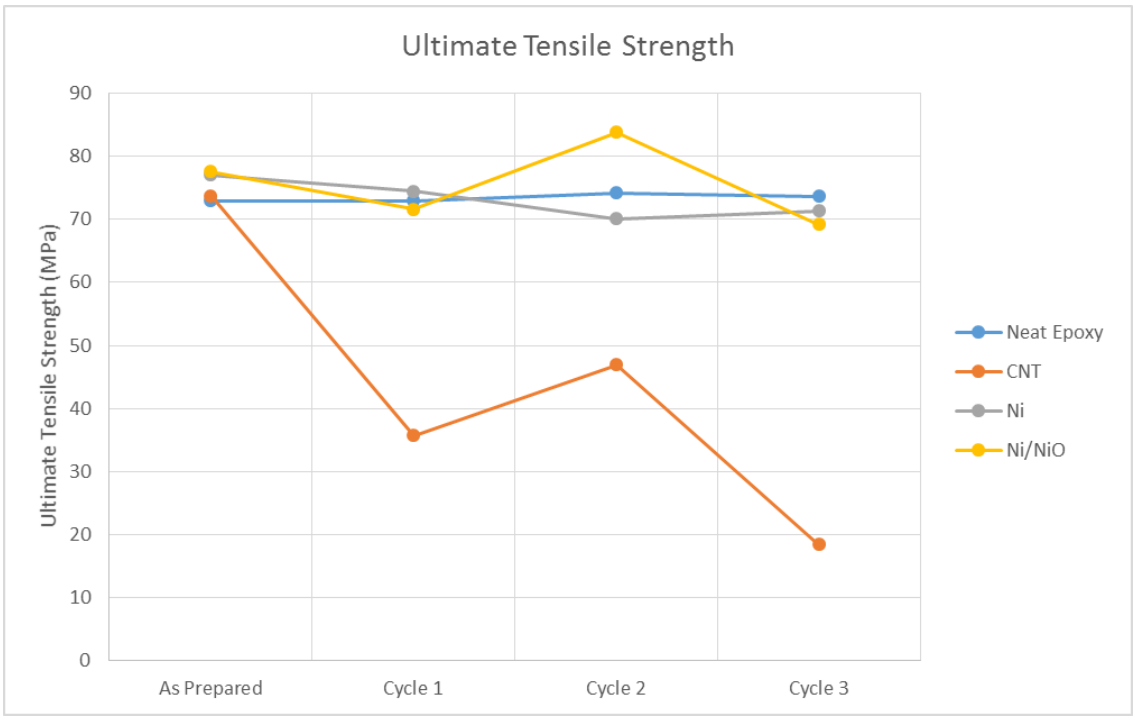

Figure 29. Graph of Neat epoxy, CNT, Ni and NiO Ultimate Tensile Strength Before and After UV and Humidity Exposure.

The CNT samples initially displayed the highest average Young's Modulus as prepared at 1131.2 MPa compared to the Ni sample, which displayed the lowest Young's Modulus of 769.8 MPa. After just one cycle in the QUV however, the CNT sample showed the most dramatic decrease in Young's Modulus to 638.6 MPa and was the lowest of the four samples. The Ni sample showed the least dramatic drop in Young's

modulus to 715.8 MPa. After the second cycle, the Young's modulus remained relatively consistent for the neat epoxy and Ni/NiO samples. The Young's Modulus increased for the Ni sample and continued to decrease for the CNT sample to 580.7 MPa. After cycle three, the Ni and CNT samples again showed the most dramatic change in Young's modulus. The Ni sample increased to the highest of the four samples at 890.7 MPa, surpassing the as prepared sample by 120.9 MPa. The Ni sample was the only sample that had a higher Young's Modulus after cycle three than as prepared. The CNT sample had the second highest Young's modulus after cycle three at 767.56 MPa, which was still 363.6 MPa below the as prepared sample (Figure 30).

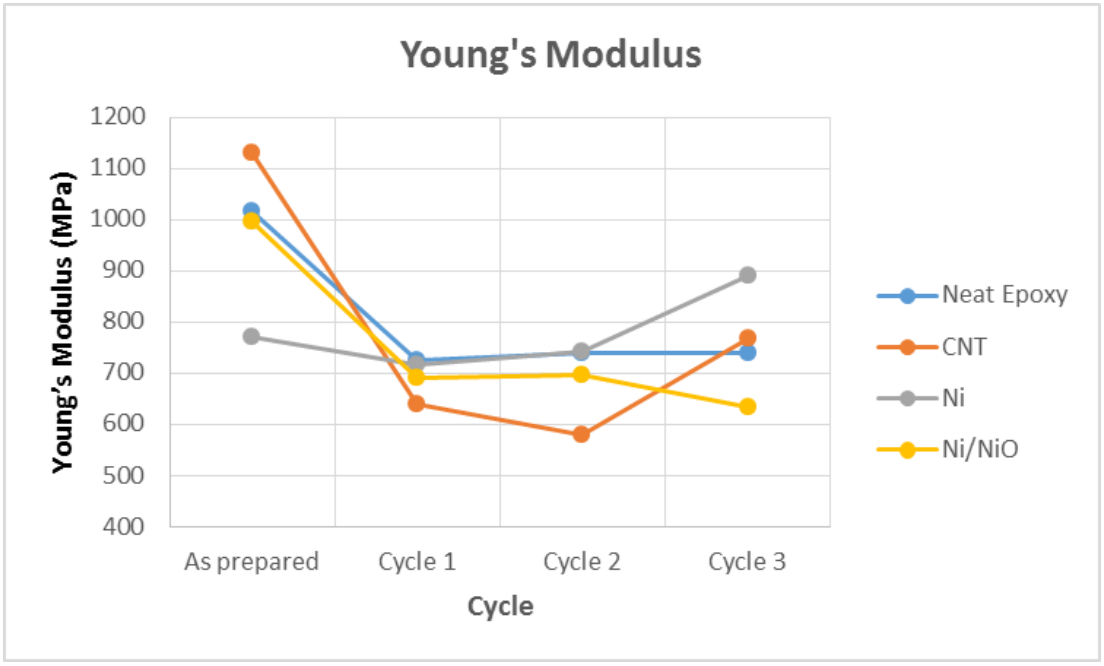

Figure 30. Graph of Neat Epoxy, CNT, Ni and NiO Samples Young's Modulus before and after UV and Humidity Exposure.

5. SHEET RESISTANCE

The Sheet Resistance was calculated for the neat epoxy, epoxy - CNT, Ni and Ni/NiO samples and is graphed in Figure 31. The resistance for the CNT sample varied the most after each cycle. After one cycle the resistance decreased from 6.01(10^8) Ohm-cm to 3.50(10^8) Ohm-cm. After the second cycle, resistance increased to just below the

as prepared sample before decreasing to the lowest resistance of 2.32(10^8) Ohm-cm after the third cycle. The neat epoxy had the highest resistance at 7.05(10^8) Ohm-cm which ultimately increased after three cycles to 7.83(10^8) Ohm-cm. Because the results vary drastically by sample, no clear conclusions can be drawn regarding the effect of humidity, UV light and nanofiller characteristics on the sheet resistance of the samples.

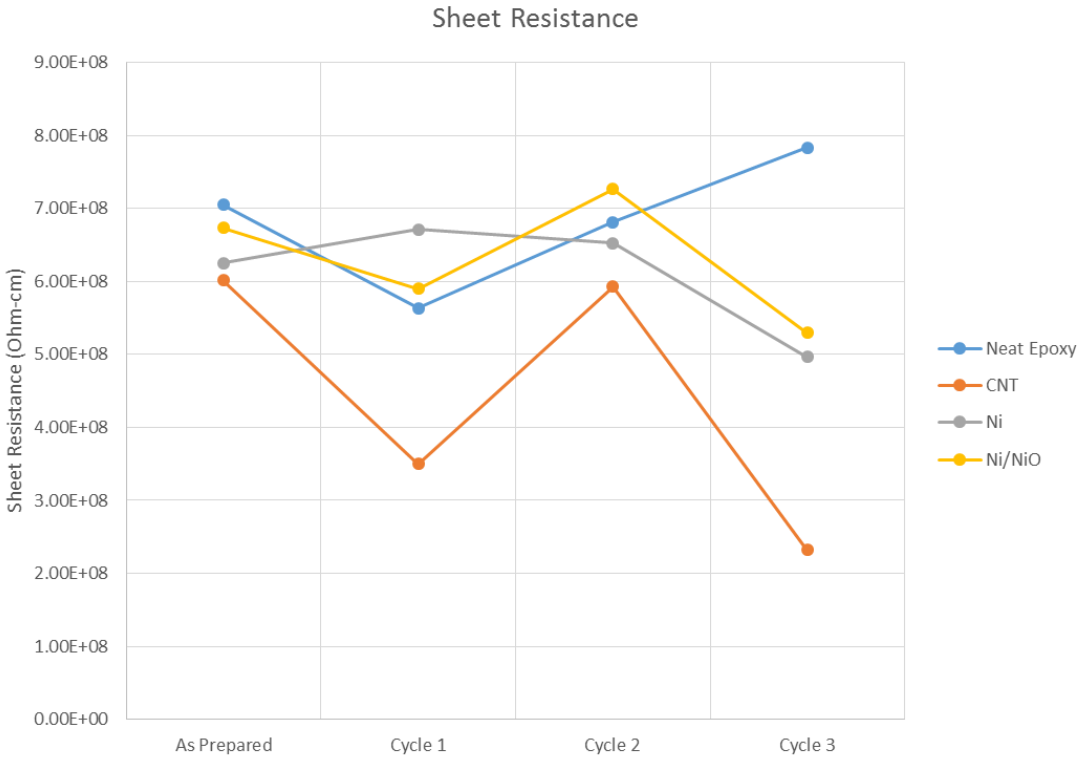

Figure 31. Sheet Resistance of Neat Epoxy, CNT, Ni, Ni/NiO samples before and after UV and Humidity Exposure.

6. WATER UPTAKE AND CHEMICAL GROUPS DETERMINED BY FOURIER TRANSFORM INFRARED SPECTROSCOPY

FTIR was conducted on the neat epoxy, epoxy - CNT, Ni and Ni/NiO nanocomposites for the as prepared samples and after cycle 1 and cycle 2. (Data for samples after cycle 3 was not collected due to time constraints). FTIR results for neat epoxy as prepared and after one and two cycles of exposure are shown in Figure 32. At 3600 cm^{-1} highly mobile free water is not present. The peaks visible at roughly 3390

cm^{-1} are associated with water uptake and the largest peak associated with cycle one is indicative of hydration and water bound to specific sites through hydrogen bonding. As seen in Figure 32, the peaks close to 830 cm^{-1} are of equal intensity for the epoxy as prepared and for cycle one. In contrast, at 1600–1650 cm^{-1} have significant changes. This same peak disappears in intensity after cycle two, which indicate a breakdown of the polymer or polymer degradation. At 1525 cm^{-1}, this peak is related to the C-C bond in the aromatic rings. The peaks located near 800–920 cm^{-1} are used as an internal standard because those are associated with epoxy groups in Figure 4. Overall, the neat epoxy shows evidence of water uptake then polymer degradation with water loss.

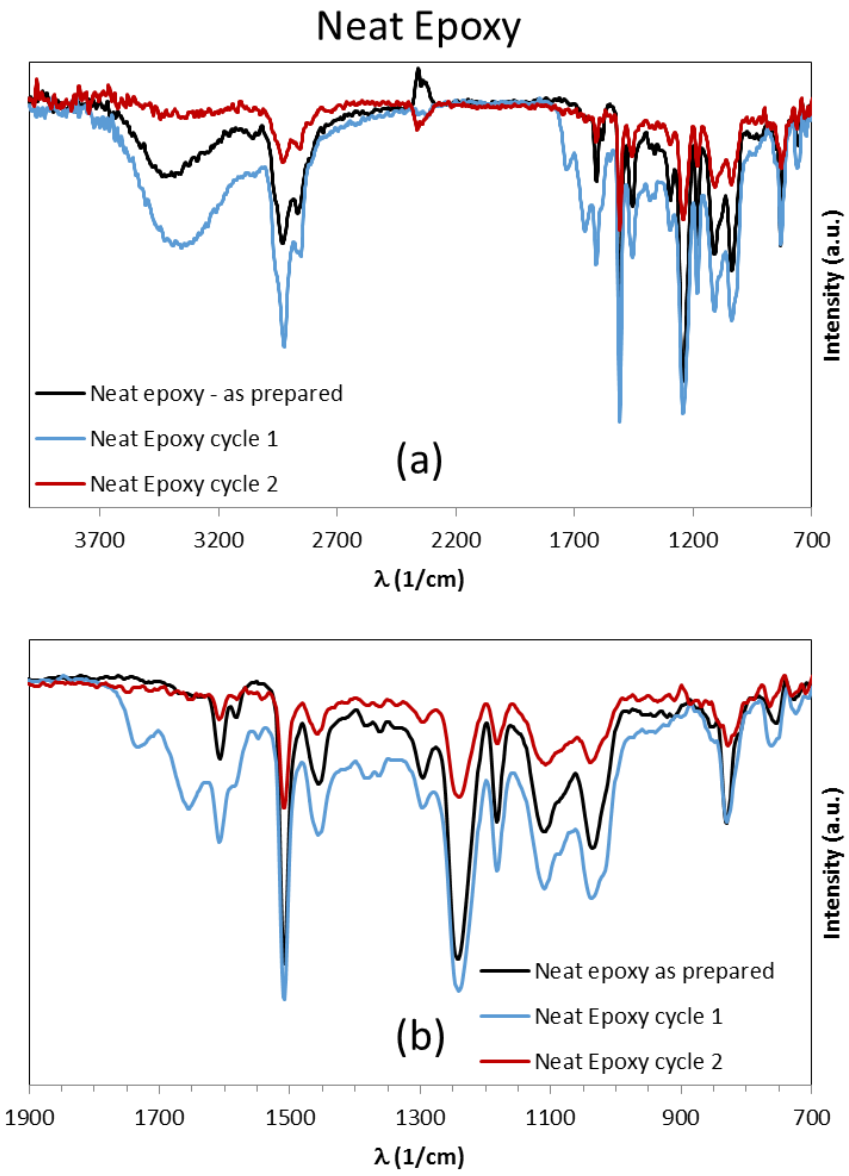

Figure 32. Neat Epoxy FTIR Before and After UV and Humidity Exposure (a) 3700–700 cm^{-1} and (b) Enlarged to 1900–700 cm^{-1}.

The FTIR data for the CNT samples in Figure 33 do not present large differences amongst the cycles. Of particular interest, the 3300 cm^{-1} peak does not change intensity meaning there is no evidence of water uptake. The QUV humidity and UV exposure cycles appear to have no effect on the CNT sample and they appear stable. Such data is consistent with visual observation and mechanical properties trends.

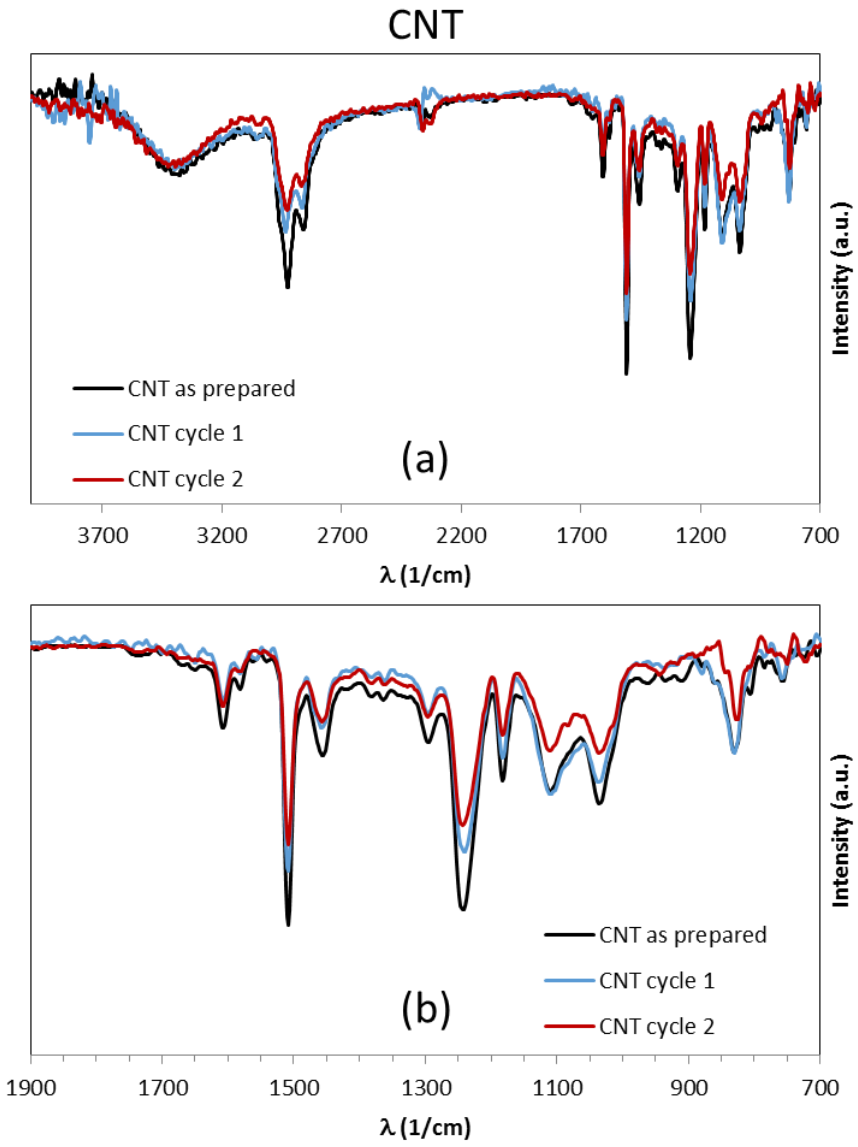

Figure 33. CNT FTIR Before and After UV and Humidity Exposure (a) 3700–700 cm^{-1} and (b) Enlarged to 1900–700 cm^{-1}.

The Ni FTIR data is displayed in Figure 34. The enlarged peak at 3300 cm^{-1} for cycle one, is evidence of hydration while the reduced size of the peak for cycle two indicates a loss of water.

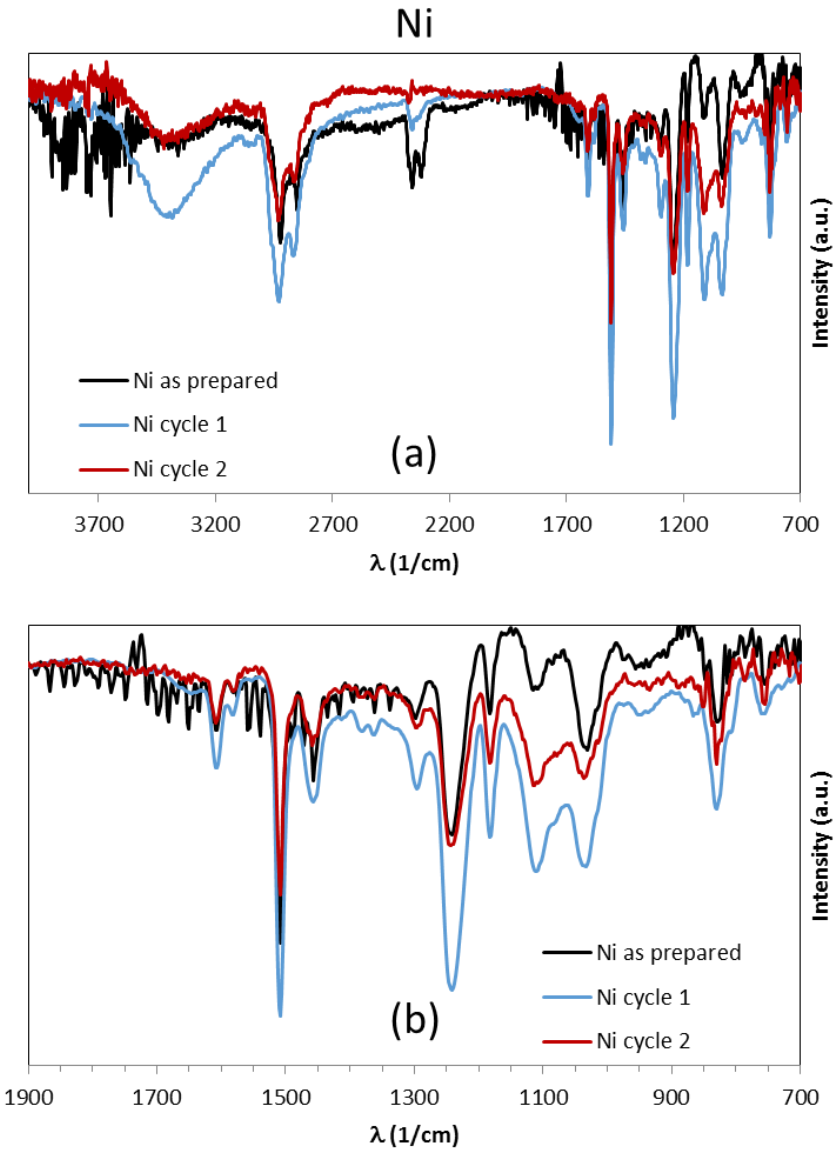

Figure 34. Ni FTIR Before and After UV and Humidity Exposure (a) 3700–700 cm^{-1} and (b) Enlarged to 1900–700 cm^{-1}.

Figure 35 shows FTIR results for Ni/NiO. The cycle two peak located near 800–920 cm^{-1}, which indicates an internal standard, is significantly larger, which excludes this data from further analysis. Also, the enlarged peak at 3300 cm^{-1} for cycle 2 indicates water uptake, while the slight decrease in intensity after cycle 1 indicated dehydration.

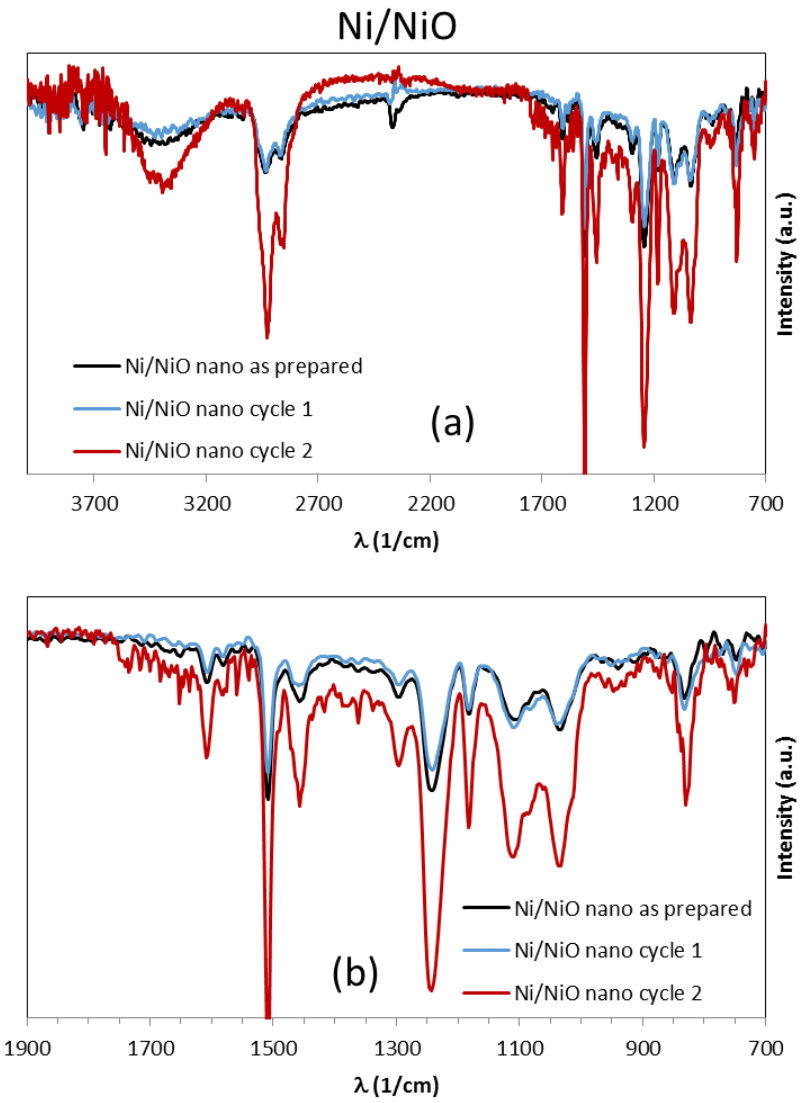

Figure 35. Ni/NiO FTIR Before and After UV and Humidity Exposure (a) 3700–700 cm^{-1} and (b) Enlarged to 1900–700 cm^{-1}.

A comparison of the four samples as prepared and after cycle 2 is presented in Figure 36 and Figure 37. Before any weather exposure, the neat epoxy and CNT samples show relatively identical peaks, as seen in Figure 36. The samples show a similar internal standard peak but the Ni and Ni/NiO samples appear to be more impacted. After cycle 2, at the 2300 cm^{-1} peak, the Ni and Ni/NiO samples show an inverted intensity compared to prior to exposure.

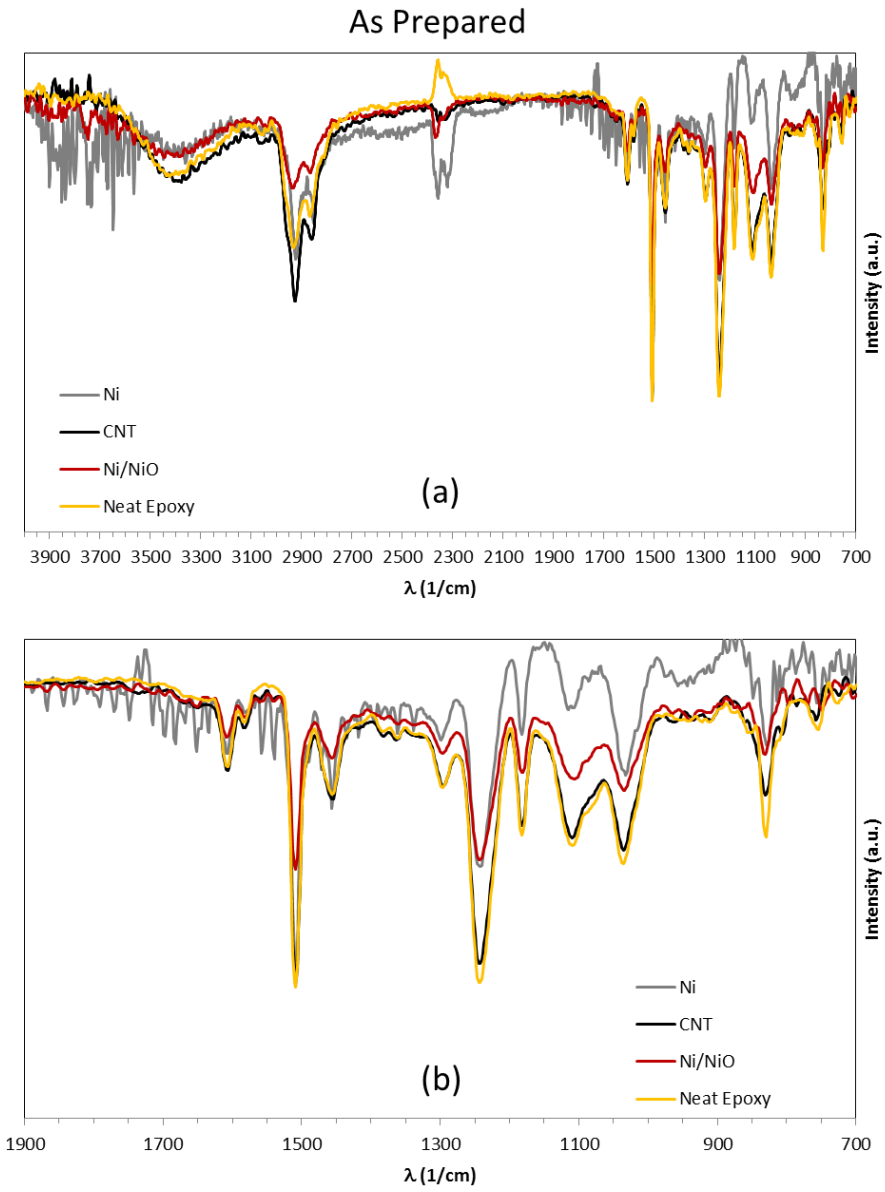

Figure 36. As Prepared FTIR Results for Ni, CNT, Ni/NiO and Neat Epoxy (a) 3700–700 cm^{-1} and (b) Enlarged to 1900–700 cm^{-1}.

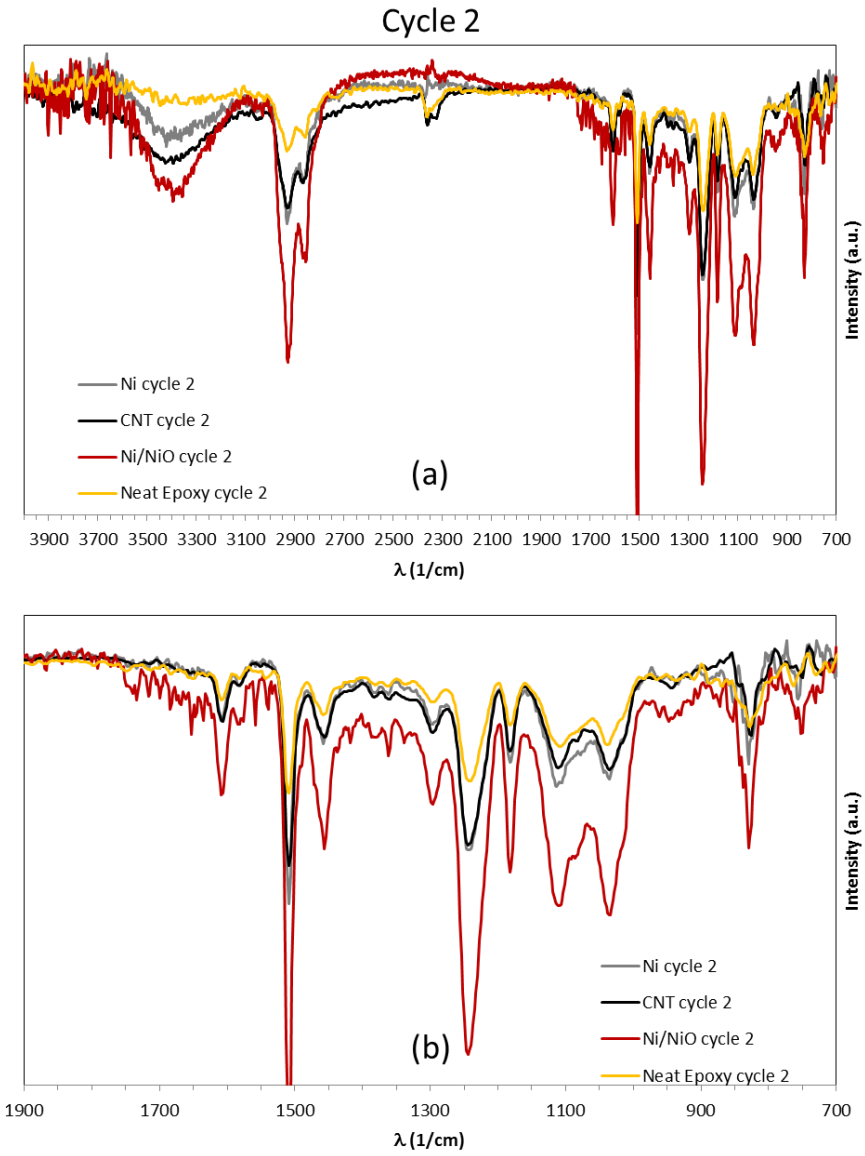

Figure 37. FTIR results for Ni, CNT, Ni/NiO and Neat Epoxy after Two Cycles of UV and Humidity Exposure (a) 3700–700 cm^{-1} and (b) Enlarged to 1900–700 cm^{-1}.

C. DISCUSSION

The neat epoxy and all nanocomposites were each severely degraded by cyclic exposure of UV and humidity. An FTIR analysis showed that samples became hydrated and dehydrated after specific cycles or that there was no evidence of water uptake in the case of the CNTs. The tensile tests were mostly in agreement with the FTIR analysis,

revealing that each sample eventually became brittle, an effect associated with photochemical aging.

A similar study was conducted by Kumar et al. [15], which analyzed the degradation of carbon fiber-reinforced epoxy composites. The study found that samples exposed to cycles of UV and humidity (similar to what was conducted in this study) decreased in weight after 125 hours and the samples continuously lost weight with an overall loss of 1.25% after 1000 hours. [15] Kumar et al. [15] determined that "UV radiation and condensation operate in a synergistic manner that leads to extensive matrix erosion, matrix microcracking, fiber debonding, fiber loss and void formation." In this thesis, the FTIR analysis did show period of hydration for the neat epoxy, Ni and Ni/NiO samples. The FTIR analysis of the CNT samples had no indication of water uptake after any cycle, and the neat epoxy and Ni samples showed signs of dehydration after cycle two.

Kumar et al. [15] also found that after 1000 of exposure, the transverse tensile strength decreased by 29%. In this thesis, samples were exposed to only 246 hours of cyclic UV and humidity exposure but each of the nanocomposites lost a significant percentage of ultimate tensile strength. The ultimate tensile strength of the CNT nanocomposite decreased from 73.75 MPa to 18.42 MPa, a change of over 75%, after three cycles of exposure from. The Ni and Ni/NiO nanocomposites each decreases in ultimate tensile strength by 7.4% and 10.7%, respectively. In comparison, the neat epoxy ultimate tensile strength changed by less than one hundredth of a percent. Thus, the presence of CNT fillers makes the epoxy resin more resistant to humid conditions but show greater impact to UV degradation since, despite less pronounced changes in color, the composite becomes more likely to fail in a brittle manner.

Hussain et al. [26] offered some conclusions regarding the processing of CNT nanocomposites, which may explain the CNT nanocomposites poor mechanical performance. CNT's tend to agglomerate due to the Van der Waals forces between the individual nanotubes, according to Hussain et al. [26]. In addition, proper dispersion facilitates "load transfer" between the polymer and the nanofiller and creates a path for conduction of electrical and thermal energy [26]. This offers an explanation for the lack

of load transfer and thus the significant decrease in ultimate tensile strength of the CNT nanocomposite in this study, since the dispersion of CNT in the epoxy did not seem to produce very homogeneous samples. Also, the sheet resistance of the CNT nanocomposite showed little difference from the neat epoxy or the other nanocomposites. In addition to even dispersion, the orientation of the nanofiller leads to more efficient load and energy transfer.

THIS PAGE INTENTIONALLY LEFT BLANK

IV. RESULTS AND DISCUSSION: EPOXY WITH NANOFILLERS AND METALLIC BACKING

A. VISUAL RESULTS

As mentioned in the experimental methods chapter, a set of nanocomposite samples were adhered to metal sheets and those subjected to humidity, UV and salt fog exposure. Images of the metallic backed samples were taken after each cycle of exposure and the salt fog and QUV samples were compared. The most notable differences are seen between the salt fog and QUV neat epoxy samples, Figure 38. The salt fog samples maintained their original translucent color while the QUV samples showed the sample gradient yellowing affect seen in the non-metallic backed samples. The CNT QUV samples showed slight discoloration after the second and third cycles in contrast the salt fog samples maintained their glossy surface after all cycles of exposure. In Figure 39, both the Ni and Ni/NiO salt fog samples experienced some dulling in the as prepared pure black samples. After one QUV cycle, the Ni/NiO sample showed immediate dulling in the surface, which was spread evenly across the surface. The Ni QUV sample in comparison showed little changes in the surface after exposure. However, the most significant observation is the pronounced delamination of the metal–epoxy interface.

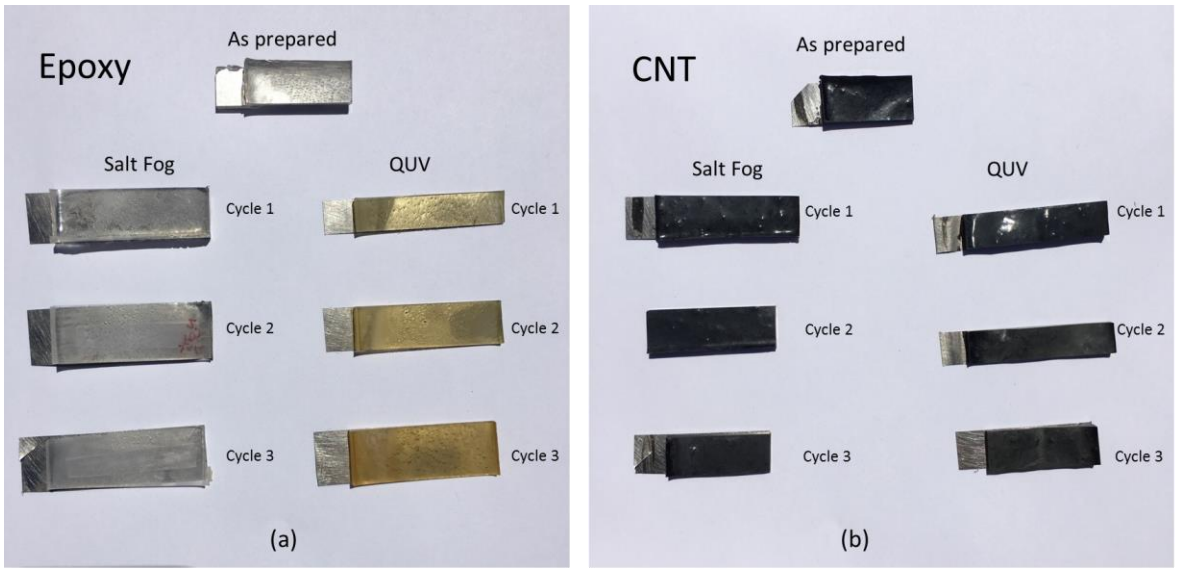

Figure 38. Salt Fog and QUV comparison for Metal Backed (a) Epoxy and (b) CNT Samples Prior to Exposure and After Each Cycle of Exposure.

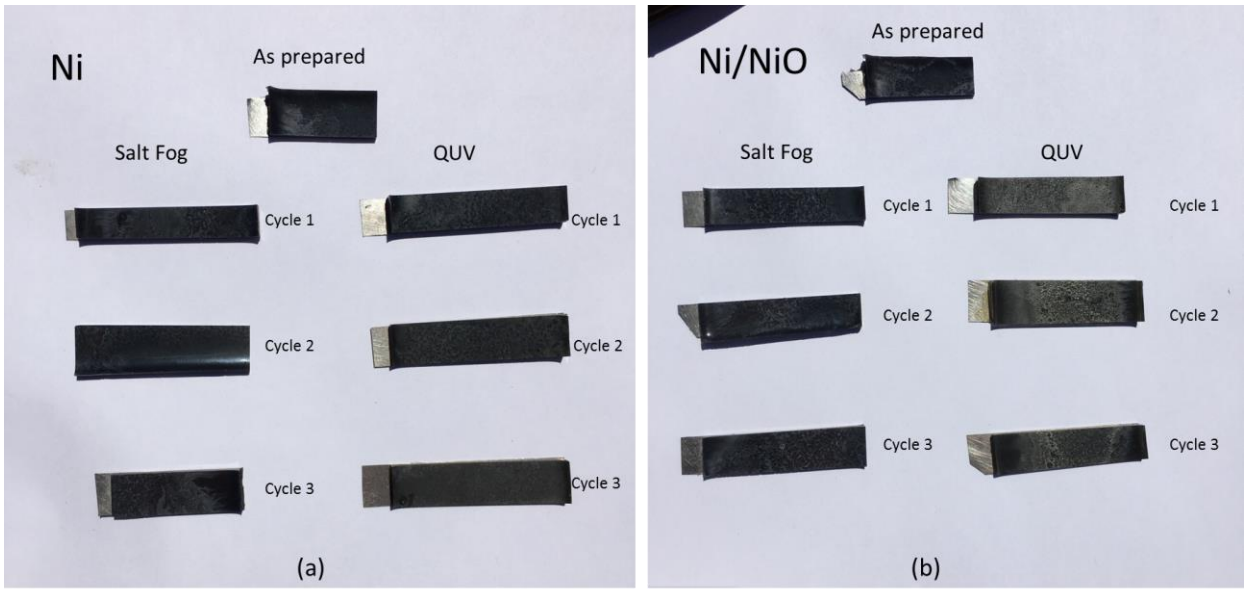

Figure 39. Salt Fog and QUV comparison for Metallic Backed (a) Ni and (b) Ni/NiO Samples Prior to Exposure and After Each Cycle of Exposure.

B. SEM

SEM images were taken of the CNT and Ni/NiO metallic backed samples as prepared and after cycle two of QUV exposure of the CNT sample and cycle three for the Ni/NiO sample. The reason for the study was to determine if any form of corrosion was detected in the epoxy or composite–metal interfaces. Delamination occurred to some degree in all samples regardless of the cycles of exposure or the nanofiller used to create the epoxy. Other than delamination, no dramatic changes were seen among the sample on the metallic backing so only a select few SEM images are presented and no other microstructural analysis was performed.

Complete separation of the CNT epoxy from the metallic backing after the third cycle precluded it from further analysis as seen in the images in Figure 40. and Figure 41. Delamination occurred in both CNT samples. In the images after cycle two, the microstructure of both the metallic backing and CNT epoxy is visible. Also, noticeable is the disruption in the CNT epoxy at the interface, which is mirrored in the stainless steel and alters the microstructure in the surrounding area.

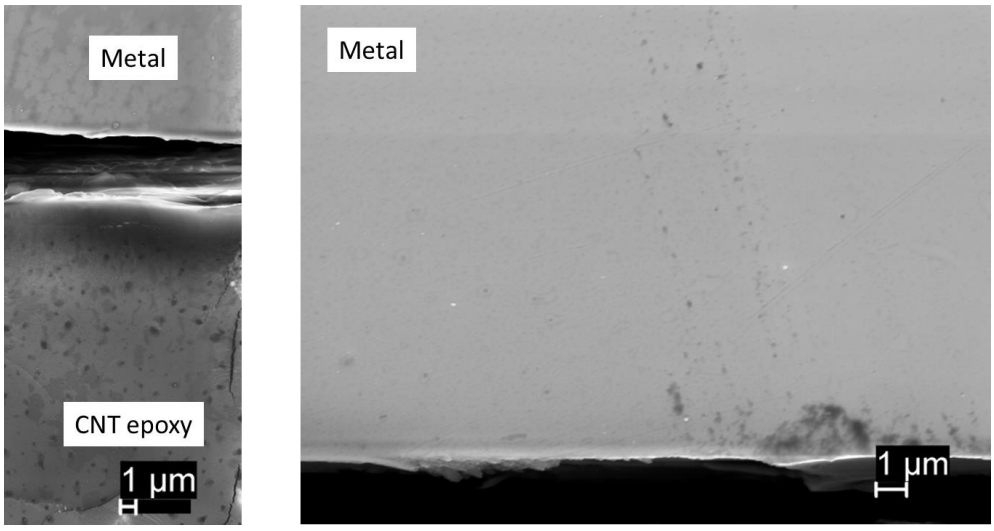

Figure 40. SEM Images of as Prepared CNT with Metallic Backing Showing Delamination.

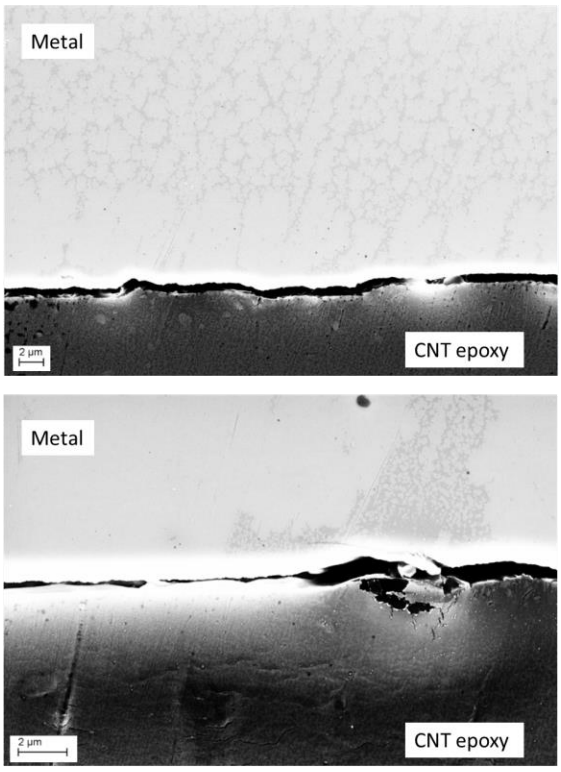

Figure 41. SEM image of CNT with Metallic Backing after Cycle 2 Showing Microstructure and Disruption at the Interface.

The SEM images in Figure 42. Figure 43. show delamination between the metallic backing and the Ni/NiO composite. In the as prepared sample, the profile of the metallic backing is mirrored in the Ni/NiO epoxy. Also, noticeable is the shifting of the microstructural layers in the stainless steel in the second image. In both as prepared images, the metallic backing shows an uneven surface at the interface.

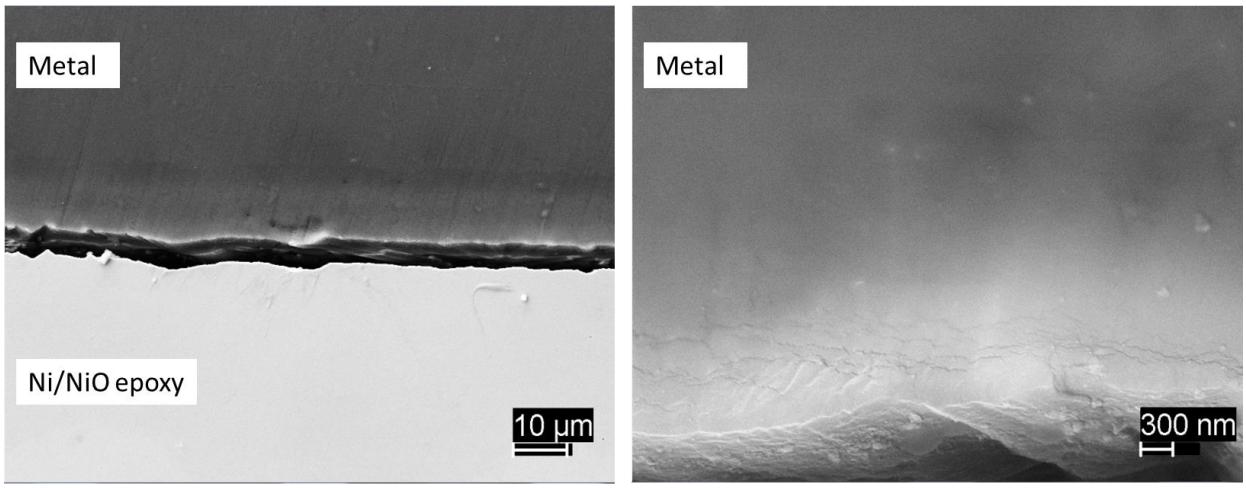

Figure 42. SEM Image of as Prepared Ni/NiO with Metallic Backing Showing Shifting of Microstructural Layers.

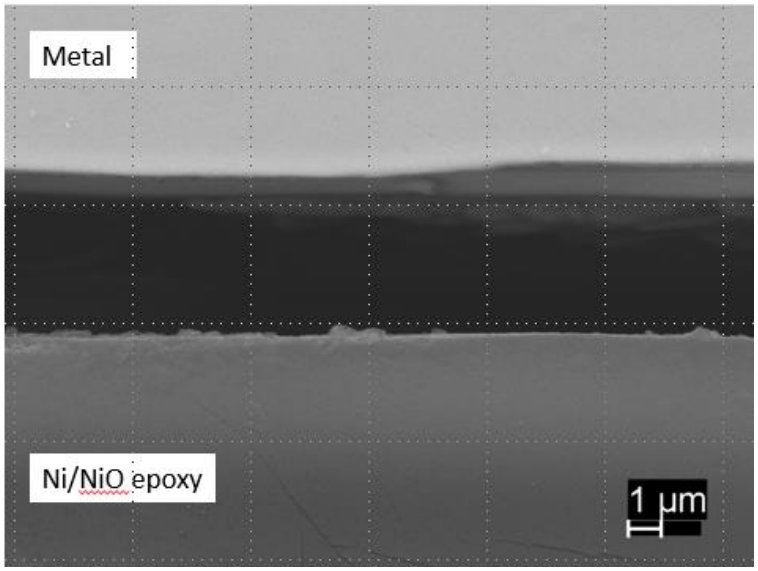

Figure 43. SEM images of Ni/NiO with Metallic Backing after Cycle 2 Showing Complete Delamination.

THIS PAGE INTENTIONALLY LEFT BLANK

V. CONCLUSION

This study aimed to characterize the change in properties that nanocomposites suffer as result of environmental factors. Epoxy resin and composites containing nano-fillers were exposed to augmented weather conditions (UV light, humidity in the form of condensation and salt fog). Some of the milestones achieved are listed below.

This thesis successfully created protocols for the fabrication, exposure, testing and comparison of neat epoxy and nanocomposites with a variety of nanofillers.

Samples were prepared using epoxy resin and 1 % loadings of SiO_2, CNTs, Ni and Ni/NiO nanoparticulates. The samples underwent 246 hours, split into three cycles, of augmented weather exposure and the effects were characterized through visual analysis, optical microscopy, microhardness, tensile tests, sheet resistance, Fourier Transform Infrared Spectroscopy and SEM. Overall, the nanocomposites showed dramatic changes to their mechanical and structural characteristics.

Through visual analysis, neat epoxy yellowed after one cycle of exposure to UV and humidity while the FTIR analysis had signs of photochemical aging and polymer degradation after a two cycles. The Vickers hardness slightly increased throughout the time of exposure with a 15.9% increase after two cycles. A stress-strain analysis had indications of slight water uptake after cycle one due to an increase in toughness. Overall, the average ultimate tensile strength of three samples, over the course of three cycles, showed a minor increase of 1.0% to 73.7MPa. Additionally, optical microscopy images revealed surface cracks after the third cycle, which would agree with dehydration after two cycles. This agreed with the FTIR results describing an increase in water uptake after cycle one and a decrease after cycle two.

The CNT nanocomposite showed only minor surface cracks after the third cycle of exposure to UV and humidity compared to the neat epoxy. Similarly, there were only minor changes in the color of the sample. This is in agreement with the FTIR analysis, which showed no evidence of polymer degradation due to water uptake. However, the CNT-epoxy samples did show the effects of photochemical aging. For example, after

cycle one, the shape of the stress strain graph indicated brittle failure, which continued for the remaining cycles. The ultimate tensile strength decreased by over 75.6% over the course of three cycles but the hardness increased by 37.2%. This lack of water uptake may have resulted in continuous decrease in toughness, strain and tensile strength of the nanocomposite, exacerbating the UV light damage and consequent rise in temperature.

The Ni nanocomposite exhibited similar color change as the CNT sample but experienced larger surface cracks after the third cycle of UV and humidity exposure. Comparatively, the Ni sample had the greatest increase in hardness after the first and third cycle, with an overall increase of 51.8% in Vickers hardness. Tensile tests showed the second smallest loss in overall tensile strength of 7.4% to 71.3 MPa; however, the samples had low toughness after the third cycle. In addition, the FTIR analysis showed a water loss after cycle two. Thus, the Ni nanocomposite specimen presented degradation linked both to water uptake and loss and UV effects.

Similar to the Ni and CNT nanocomposites, the Ni/NiO samples revealed little color change after three cycles of exposure to UV and humidity and had surface cracks similar to the Ni samples. The Ni/NiO nanocomposite had the second largest increase in hardness after cycle three of 36.1% to 19.96 HV. The FTIR showed dehydration of the sample after cycle one but rehydration after cycle two. Similarly, the stress-strain graph displayed an increase in toughness indicating hydration after the second cycle. The ultimate tensile strength decreased 10.7% over the course of three cycles of exposure to 69.2 MPa. Finally, the toughness decreased after cycle three illustrating drying of the sample and loss of ductility.

All samples appear highly susceptible to UV degradation. Nanocomposites with Ni, Ni/NiO and SiO2 fillers swell and absorb water with a minimal number of hours of exposure. Nanocomposites with a CNT filler are more resistant to humidity but degrade more due to UV degradation.

Finally, metallic backed CNT and Ni/NiO samples were examined using SEM. All samples, including the neat epoxy and Ni samples, were delaminated to some degree after one cycle of exposure. Both the CNT and Ni/NiO SEM images indicated shifting in

the microstructural layers of the stainless steel. Also, the profile of the metallic backing was mirrored in the nanocomposite. Finally, the delamination revealed an uneven surface at the interface.

Overall, it is recommended that nanocomposites are tested under working conditions for longer periods of exposure. A thorough characterization of nanocomposites should be conducted prior to any defense applications.

Future work should conduct a literature research to determine new epoxy formulations, which have chemical groups less likely to be affected by humidity or UV light. This study only examined one of many different types of epoxy resins.

A protocol for a more effective dispersion of the fillers should be determined. More effective dispersion is expected to produce homogeneous nanocomposites. This should lead to more consistency in the data and smaller standard deviation values for tensile strength and hardness.

An ASTM standard tensile test specimen with a longer gauge length should be employed in order to generate tensile test data that can be compared to other studies.

In addition, longer UV, humidity and salt fog exposure times should be used for the samples containing metal backing in order to observe the long-term corrosion effects of using diverse fillers.

THIS PAGE INTENTIONALLY LEFT BLANK

LIST OF REFERENCES

[1] R. V. Kurahatti et al., "Defence applications of polymer nanocomposites," *Def. Sci. J.,* vol. 60, pp. 551–563, Sep 2010.

[2] D. Ciprari, K. Jacob and R. Tannenbaum, "Characterization of polymer nanocomposite interphase and its impact on mechanical properties," *Macromolecules,* vol. 39, pp. 6565–6573, Sep 19, 2006.

[3] X. Li *et al.,* "Nanoscale structural and mechanical characterization of a natural nanocomposite material: The shell of red abalone," *Nano Lett.,* vol. 4, pp. 613–617, Apr 2004.

[4] H. Kuan *et al.,* "Synthesis, thermal, mechanical and rheological properties of multiwall carbon nano tube/waterborne polyurethane nanocomposite," *Composites Sci. Technol.,* vol. 65, pp. 1703–1710, Sep 2005.

[5] K. Haraguchi and H. Li, "Mechanical properties and structure of polymer-clay nanocomposite gels with high clay content," *Macromolecules,* vol. 39, pp. 1898–1905, Mar 7, 2006.

[6] L. Shi *et al.,* "Mechanical properties and wear and corrosion resistance of electrodeposited Ni-Co/SiC nanocomposite coating," *Appl. Surf. Sci.,* vol. 252, pp. 3591–3599, Mar 15, 2006.

[7] F-35A Lightning II. (n.d.). Military.com [Online]. Available: http://www.military.com/equipment/f-35a-lightning-ii. Accessed Mar 13, 2017.

[8] What's So Special about the Nanoscale? (n.d.). National Nanotechnology Initiative [Online]. Available: https://www.nano.gov/nanotech-101/special. Accessed Mar. 8, 2017.

[9] S. Iijima, "Helical Microtubules of Graphitic Carbon," *Nature,* vol. 354, pp. 56–58, Nov 7, 1991.

[10] J. Ging *et al.,* "Development of a conceptual framework for evaluation of nanomaterials release from nanocomposites: Environmental and toxicological implications," *Sci. Total Environ.,* vol. 473, pp. 9–19, MAR 1, 2014.

[11] R. Asmatulu *et al.,* "Effects of UV degradation on surface hydrophobicity, crack, and thickness of MWCNT-based nanocomposite coatings," *Prog. Org. Coat.,* vol. 72, pp. 553–561, Nov 2011.

[12] T. Nguyen *et al., Network Aggregation of CNTs at the Surface of Epoxy/MWCNT Composite Exposed to UV Radiation.* Boca Raton; 6000 Broken Sound Parkway NW, STE 300, Boca Raton, Fl., 33487-2742 USA: CRC Press-Taylor & Francis Group, 2009.

[13] E. Yousif and R. Haddad, "Photodegradation and photostabilization of polymers, especially polystyrene: review," *SpringerPlus,* vol. 2, pp. 398, 2013.

[14] F. Bottino *et al.,* "Chemical modifications, mechanical properties and surface photo-oxidation of films of polystyrene (PS)," *Polym. Test.,* vol. 23, pp. 405–411, Jun 2004.

[15] H. Kumar, R. Singh and T. Nakamura, "Degradation of carbon fiber-reinforced epoxy composites by ultraviolet radiation and condensation," *J. Composite Mater.,* vol. 36, pp. 2713–2733, 2002.

[16] S. Bocchini, A. Di Blasio and A. Frache, "Influence of MWNT on Polypropylene and Polyethylene Photooxidation," *Eurofillers,* vol. 301, pp. 16–22, 2011.

[17] M. Gonzalez, J. Cabenelas and J. Baselga, "Applications of FTIR on epoxy resins - identification, monitoring the curing process, phase separation and water uptake," in *Infrared Spectroscopy - Materials Science, Engineering and Technology*, Theophanides Theophile, Ed. InTech, 2012.

[18] M. R. Loos *et al.,* "Effect of Carbon Nanotubes Addition on the Mechanical and Thermal Properties of Epoxy Matrices," *Mater. Res. -Ibero-Am. J. Mater.,* vol. 11, pp. 347–352, Jul-Sep 2008.

[19] V. Choudhary and A. Gupta, "Polymer/carbon nanotube nanocomposites," in *Carbon Nanotubes - Polymer Composites*, S. Yellampalli, Ed. InTech, 2011.

[20] P. Guo *et al.,* "Fabrication and mechanical properties of well-dispersed multiwalled carbon nanotubes/epoxy composites," *Composites Sci. Technol.,* vol. 67, pp. 3331–3337, Dec 2007.

[21] M. Moniruzzaman and K. I. Winey, "Polymer nanocomposites containing carbon nanotubes," *Macromolecules,* vol. 39, pp. 5194–5205, Aug 8, 2006.

[22] Silicon Dioxide (SiO2) Nanopowder / Nanoparticles (SiO2, 99+%, 20–30nm, amorphous). (n.d.). U.S. Researcher Nanomaterials, Inc. [Online]. Available: http://libguides.nps.edu/citation/ieee#webnoauthordate. Accessed Feb 9, 2017.

[23] MWCNTs (>95%, OD: 10–20 nm) (n.d.). U.S. Researcher Nanomaterials Inc. [Online]. Available: http://www.us-nano.com/inc/sdetail/224. Accessed Feb 9, 2017.

[24] *Nickel (Ni) Nanoparticles / Nanopowder (Ni, 99.9%, 20nm, carbon coated, metal basis) (n.d.). U.S. Researcher Nanomaterials, Inc. [Online]. Available: http://www.us-nano.com/inc/sdetail/171. Accessed Feb 9, 2017.

[25] P. Brennan, "Improved UV light source enhances correlation in accelerated weathering," Q-Lab Corporation, Westlake, Ohio, Tech. Rep. LU-8003, 2011.

[26] F. Hussain *et al.*, "Review article: Polymer-matrix nanocomposites, processing, manufacturing, and application: An overview," *J. Composite Mater.*, vol. 40, pp. 1511–1575, Sep 2006.

THIS PAGE INTENTIONALLY LEFT BLANK

INITIAL DISTRIBUTION LIST

1. Defense Technical Information Center
   Ft. Belvoir, Virginia

2. Dudley Knox Library
   Naval Postgraduate School
   Monterey, California